University of Nevada, Reno

Morphologic signatures of autogenic waterfalls:

A Case Study in the San Gabriel Mountains, California

A thesis submitted in partial fulfillment of the requirements

for the degree of Master of Science in Geology

By

Erika L. Groh

Thesis Advisor: Dr. Joel S. Scheingross

August 2021

THE GRADUATE SCHOOL

We recommend that the dissertation
prepared under our supervision by

ERIKA GROH

entitled

Morphologic signatures of autogenic waterfalls: A case study in the San Gabriel Mountains, California

be accepted in partial fulfillment of the
requirements for the degree of

Master of Science

Joel Scheingross, Ph.D.
Advisor

Scott McCoy, Ph.D.
Committee Member

Andrew Zuza, Ph.D.
Committee Member

Amanda Keen-Zebert, Ph.D.
Committee Member

Joanna Blaszczak, Ph.D.
Graduate School Representative

David W. Zeh, Ph.D., Dean
Graduate School

August, 2021

ABSTRACT

Waterfalls are powerful agents of geomorphic work as they can erode at different rates than surrounding reaches, thereby setting the pace of landscape evolution. Waterfalls can form due to external perturbation of river base level, lithologic heterogeneity, and internal feedbacks (i.e., autogenic dynamics). While criteria for identification of waterfalls formed by lithologic heterogeneity and external perturbation are well documented, there has been no systematic description of how to identify self-formed (autogenic) waterfalls, therein limiting assessment of the ubiquity of self-formed waterfalls and their influence on past environmental forcing encoded in topography. Based on the assumption that autogenic waterfalls form from a specific type of bedrock bedform known as cyclic steps, we propose that autogenic waterfalls should form in series with waterfall height and spacing between waterfalls set primarily by channel slope. We use high resolution topography in the San Gabriel Mountains, California, to identify 360 waterfalls and show that waterfalls tend to form at channel slopes >3%, coinciding with the onset of Froude supercritical flow, and that the waterfall height to spacing ratio increases with channel slope; consistent with cyclic step theory and previous laboratory experiments. Our results imply that in unglaciated mountain ranges with relatively uniform rock strength, the majority of waterfalls may be autogenic in origin.

ACKNOWLEDGEMENTS

No one accomplishes anything alone and I have been lucky enough to have a village of people who have helped me get to this point. I especially would like to thank my advisor, Dr. Joel Scheingross, for going above and beyond in his support and advice, not only for my research and graduate school, but also for my future career and life in general. I have learned a tremendous amount from him about how to be a successful scientist and truly appreciate the time and effort he put in to helping me succeed. I would also like to thank my geomorphology research group (Alison Cramer, David Cavagnaro, Ingrid Suter, Nathan Delgado, Scott Fehan, and Sophie Rothman) for their constant support and encouragement as well as their help with my research and field work. Having a close-knit group to celebrate the highs and support me through the lows was so important to me and I will forever be grateful for that. I also would like to thank the entire Geology Department for the sense of community and positivity that I felt from the moment I started graduate school. Lastly, thank you to my wonderful family (Susan, Ron, and Kadie Groh) and my partner (Michael Say) for always encouraging me and loving me. I also thank Dr. Ellen Wohl for sharing Nahal Yael data and acknowledge National Science Foundation funding to J.S.S. via EAR-1946342.

TABLE OF CONTENTS

LIST OF TABLES

LIST OF FIGURES

Supplemental Figures

1.0 INTRODUCTION

Waterfalls can set the pace of landscape evolution, in cases eroding slowly relative to rock uplift rates creating large escarpments, while in other cases, eroding faster than uplift rates, carving bedrock canyons and altering river slope (DiBiase et al., 2015). In mountainous areas, waterfalls can drive the headward retreat of locally steepened channel reaches, termed knickzones (e.g., Crosby and Whipple, 2006; Berlin and Anderson, 2007). Predicting the influence of waterfalls on landscape evolution and interpreting how Earth history is encoded in river profiles requires a mechanistic understanding of waterfall formation and the ability of waterfalls to modulate knickzone retreat (e.g., Whittaker, 2012; Scheingross et al., 2020).

Waterfall and knickzone formation is commonly associated with pulses of uplift, changes in sea level, glaciation, and/or lithologic heterogeneity (e.g., Whittaker and Boulton, 2012; Forte et al., 2016; Mackey et al., 2014; Valla et al., 2010); however, except in rare cases (Yanites et al., 2010; Malatesta and Lamb, 2018), it is unlikely that each individual waterfall can be attributed to a specific external perturbation or lithologic control. Therefore, there must be another process forming waterfalls. An alternative hypothesis is that waterfalls self-form (i.e., they form autogenically) due to feedbacks between erosion, sediment transport, and flow hydraulics (Scheingross et al., 2019). Experiments and theory show that bedrock channels subject to Froude supercritical flow can develop a series of repeating, low-amplitude bedrock steps separated by hydraulic jumps, commonly referred to as cyclic steps (e.g., Izumi et al., 2017; Baynes et al., 2018; Grimaud et al., 2016; Yokokawa et al., 2013). Feedbacks between sediment cover and

erosion between adjacent pools allow cyclic steps to grow in height, forming waterfalls (Scheingross et al., 2019).

Experiments have documented cyclic step and autogenic waterfall formation (e.g., Brooks, 2001; Baynes et al, 2018; Scheingross et al., 2019; Yokokawa et al., 2016), yet there are few field studies documenting cyclic steps in bedrock (Duckson and Duckson, 1995; Wohl and Grodek, 1994). The lack of quantitative field data verifying the existence and ubiquity of autogenic waterfalls fundamentally limits our ability to explore the interplay of internal dynamics and external forcing in river networks (Scheingross et al., 2020). Here, I address this knowledge gap by asking three questions: 1) Do autogenic waterfalls form in nature? 2) Do autogenic waterfalls have a unique morphologic signature? And 3) Does autogenic waterfall morphology differ between steady state and transient landscapes? To answer these questions, I define autogenic waterfall identification criteria, and compare these criteria to 360 waterfalls in the San Gabriel Mountains (SGM), California and previous studies of cyclic steps in flume experiments and field surveys.

1.1 Criteria for Autogenic Waterfall Identification

I propose that autogenic waterfalls are bedrock bedforms that form via cyclic step growth. As such, I expect autogenic waterfalls to have a unique morphology and spatial distribution relative to externally- or lithologically-forced waterfalls. Following cyclic step theory (Izumi et al., 2017), I expect the spacing between autogenic waterfalls and waterfall height to be set by the ratio of fluvial sediment supply to sediment transport capacity (Q_s/Q_{sc}), which modulates fluvial bedrock erosion rates (Sklar and Dietrich,

2001), and flow Froude number (Fr). For constant Q_s/Q_{sc}, cyclic step theory predicts that step spacing increases and step height decreases with increasing channel slope (Izumi et al., 2017).

The morphodynamic instabilities leading to cyclic step formation requires Froude supercritical flow (Fr > 1), and thereby controls where autogenic waterfalls form within river networks. Under steady, uniform flow, $Fr = (S/C_f)^{1/2}$, where S is channel slope and C_f is the bed friction factor, suggesting there may be a critical slope above which autogenic waterfalls are more likely to form due to the onset of Fr > 1 flow. Field data shows that Fr > 1 flow is common for $0.03 < S < 0.07$, but Fr decreases at $S > 0.07$ because the onset of supercritical flow drives bedform formation, lowering flow velocity and returning the river to Fr < 1 flow (Palucis and Lamb, 2017) (Fig. 1). The natural function of bedforms is to act as energy dissipators. When a stream reaches unstable conditions, bedforms autogenically arise to return stability to the flow. Following this logic, if autogenic waterfalls are bedrock bedforms that form due to the presence of supercritical flow, I expect waterfalls to be absent at $S < 0.03$, begin forming at $0.03 < S < 0.07$, and be most prevalent at $S > 0.07$. For a steady state, concave-up river profile, this should manifest as an increasing occurrence of autogenic waterfalls moving upstream.

1.2 Distinguishing Autogenic from Externally-Forced Waterfalls

In contrast to the criteria discussed above for autogenic waterfall formation, I expect externally- and lithologically-forced waterfalls to have spatial distributions set by the type of forcing, rather than channel morphodynamics. For example, contrasting erosion rates between weak and hard rock can create waterfalls (e.g., Frankel et al.,

2007). However, in this case, the waterfall location and height are set primarily by spatial variations in rock strength, with channel slope playing a secondary role (Berlin and Anderson, 2009). Similarly, base-level perturbations can cause waterfalls to align with a fault trace, or, for perturbations at a river outlet, upstream propagation can cause waterfalls to cluster at similar elevations within a drainage basin (e.g., Crosby and Whipple, 2006; Wobus et al., 2006). In these cases, waterfall spacing should be more strongly set by the timing between base-level perturbations and height should be set by the fault displacement, rather than show a systematic variation with channel slope as I propose for autogenic waterfalls.

2.0 STUDY AREA AND METHODS

2.1 San Gabriel Mountains

The San Gabriel Mountains (SGM), California (Fig. 2) are an ideal locale to test for autogenic waterfall formation. The range has never been glaciated, it is dominated by crystalline rocks with similar rock strength due to extensive tectonic fracturing during exhumation (DiBiase et al., 2010; Neely et al., 2019), and precipitation varies by only ~0.3 m/yr across our study region (PRISM). The SGM has two large fault systems; the Sierra Madre Cucamonga fault zone (SMFZ) to the south and the San Gabriel fault zone (SGFZ) which cuts through the center of the range (Fig. 2). In this analysis, I focused on two distinct regions of the SGM. The Central Sierra Madre Block, hereafter referred to as the Front Range (Fig. 2), has been argued to be in topographic steady state as evidenced by compatible fluvial incision rates and fission track thermochronology which show an equivalence between erosion and uplift rates since the Pliocene (Lave and Burbank,

2004). In contrast, the Big Tujunga watershed is responding to multiple pulses of uplift along a section of the SMFZ (DiBiase et al., 2015). The different tectonic histories between these adjacent areas are presumably due to spatial variation in uplift history along the SMFZ, and allow us to explore autogenic waterfall formation in steady-state (Front Range) and transient (Big Tujunga) landscapes.

2.2 Defining a Waterfall

I identified waterfalls using 1 m^2 Lidar from the SGM (OpenTopography) and river long profiles extracted using TopoToolbox (Schwanghart and Scherler, 2014). I first outlined the study watersheds in ArcMap then used TopoToolbox to extract the main stem and tributaries for each individual watershed with a threshold drainage area of 1 km^2 to define the channel head (Supplemental Code), corresponding to the local colluvial-to-fluvial channel transition (Neely and DiBiase, 2020), and similar to previous studies (DiBiase et al., 2015). The results of the river profile extraction code save the distance from the outlet, elevation, and channel slope at each pixel along the profile. Waterfalls were defined as channel reaches which sustained a local river slope >30° across 3 pixels. This defined the top (lip) and bottom (base) of potential waterfalls that matched the slope requirement. I then set a threshold waterfall step height of 1.5 m in that the vertical distance between the waterfall lip and base must be over 1.5 m (Supplemental Code). The resulting definition of a waterfall in our algorithm is a channel reach with a slope >30° over a vertical distance of 1.5 m and a drainage area >1 km^2. This automated identification method produced a river long profile with the lip and base of each waterfall indicated for the main stem and tributaries of each watershed (Fig. S1).

2.3 Removal of Human-Built Structures

The SGM are heavily populated, especially at the base of the Front Range, and are prone to catastrophic debris flows. In response, the city of Los Angeles installed concrete energy dissipation structures called check dams along many of the Front Range channels to catch sediment and protect developments near the channel outlets. Check dams and other human-built structures can be falsely identified as waterfalls using the automated method outlined above, so I manually removed them from the dataset to ensure that only natural waterfalls were included in the analysis (Table 1). I used slopeshade maps created from Lidar DEMs, as well as Google Earth imagery to identify check dams. Check dams had straight crests perpendicular to the channel (Fig. 3A) in contrast to waterfalls which often had arcuate shapes (Fig. 3B). Excluding the Santa Anita watershed, the automated method identified 56 straight-crested drops as waterfalls, and I was able to visually confirm the presence of concrete, human-made structures for 53 of these cases (Fig. 3C,D). I removed both the 53 visually-confirmed concrete structures from the analysis, as well as the 3 structures I was not able to confirm, as the morphology of structures in both of these groups was similar. In the main stem and tributaries to Santa Anita Canyon, there were greater than 40 structures that had a morphologic appearance consistent with a check dam; however, image resolution, angle, and shading from trees prevented me from confirming these as concrete structures in Google Earth imagery. I removed all tributaries with suspected check dams in Santa Anita Canyon from our analysis, thereby limiting the database to cases where I had high confidence in identification of both waterfalls and check dams.

2.4 Measurement of Waterfall Metrics

Following cyclic step theory (Parker and Izumi, 2000), I defined an autogenic waterfall unit extending from the hydraulic jump at the base of a waterfall to the hydraulic jump at the base of the next downstream waterfall (Fig. 4). This is based on the assumption that erosional signals cannot travel upstream through a hydraulic jump so each waterfall "unit" will only respond to the signals passed to it from upstream between hydraulic jumps. This also most closely matches how cyclic step experimental measurements are made. I define the waterfall unit geometry using the distance from the channel head (X) and elevation (Z), I use the subscripts L and B to define the waterfall lip and base, and subscripts *1* and *2* to define the upstream and downstream waterfalls, respectively (Fig. 4). These coordinates define the waterfall unit spacing, L_U, the waterfall height, H_{wf}, the waterfall unit slope, S_U, and the river slope (the channel reach between waterfalls), S_R:

$$L_U = X_{B2} - X_{B1} \quad (1)$$

$$H_{wf} = Z_L - Z_B \quad (2)$$

$$S_U = Z_{B2} - Z_{B1} / (X_{B2} - X_{B1}) \quad (3)$$

$$S_R = Z_{L2} - Z_{B1} / (X_{L2} - X_{B1}) \quad (4)$$

These are the primary metrics of waterfall morphology that I used to test against the criteria for identifying autogenic waterfalls.

2.5 Comparison of SGM Waterfall Metrics with Previous Studies

To test for the presence of autogenic waterfalls, I compared the above metrics from the SGM dataset with previous cyclic step laboratory experiments (Table 2). These experiments were conducted at a range of slopes and using various substrates including loose sediment, cohesive sediment, ice, and artificial bedrock (Brooks, 2001; Ashida and Sawai, 1977; Koyama and Ikeda, 1998; Scheingross et al., 2019; Taki and Parker, 2005; Yokokawa et al., 2016). The channel slope in the case of experiments was equivalent to the slope at which the flume was tilted, and the spacing between waterfalls was typically measured from hydraulic jump to hydraulic jump. Both the waterfall spacing and height were averaged for each experimental run. I also compared the SGM waterfall metrics with a previous field survey of cyclic steps in bedrock rivers (Wohl and Grodek, 1994).

2.6 Cyclic Step Survey in the Ruby Mountains, NV

To explore cyclic step and autogenic waterfall formation at an intermediate scale between laboratory experiments and river channels, I surveyed cyclic steps eroded into granitic hillslopes in the Ruby Mountains, NV (Fig. 5, Table 3). These centimeter-scale steps formed in succession on hillslopes of varying slope and aspect, and had no water flowing over them at the time of the survey. Most of the pool-like structures were partially filled with sand-sized sediment while the step-like structures had exposed bedrock. We used a tape measure to measure step height and pool length as a proxy for the spacing between steps (Fig. 5E). To measure the slope of each group of steps, I laid a level with an inclinometer across the length of steps or, if the slope changed within the group, across sections with the same slope. I also measured the slope of the hillslope next

to the steps and averaged those values with the slope of the steps to get the total average slope.

2.7 Statistical Analysis

I used the Pearson Correlation Coefficient, ρ, to test for statistical correlation between waterfall metrics and slope for the Front Range SGM, Big Tujunga SGM, cyclic step experiments, Wohl and Grodek (1994) field survey, and my field survey in the Ruby Mountains. The Pearson Correlation Coefficient states that ρ=1 and ρ= -1 for monotonic positive and negative correlations, respectively. The closer the result of the test is to 1 or -1, the more strongly the metrics are correlated with slope. I also performed a two-sample Kolmogorov-Smirnov (K-S) statistical test comparing the distribution of waterfall spacing, waterfall height, and the ratio of waterfall height to spacing for the Front Range and Big Tujunga. The K-S test compares two datasets to test whether they come from the same continuous distribution where H=0 represents the affirmative and H=1 represents the negative. The P-value represents the significance level of the correlation between the data where a lower value is more significant.

2.8 Spatial Distribution of Waterfalls and Waterfall Occurrence

To determine the ubiquity of waterfalls in nature and test for a threshold slope for autogenic waterfall formation, I examined waterfall along-channel frequency by calculating the fraction of total channel relief from waterfalls as a function of channel slope, averaged over 0.5 km of channel length. The fraction of relief from waterfalls was calculated as the sum of waterfall step heights divided by the average channel slope for each 0.5 km section.

To distinguish autogenic versus external control on waterfall formation, I mapped waterfall spatial distribution and qualitatively examined the correlation between waterfalls and faults. I also examined the along-channel waterfall distribution by calculating the non-dimensional distance (X_{ND}) of waterfalls as X_L / L_R where X_L is the distance of the waterfall from the channel outlet and L_R is the total channel length from outlet to channel head. This allowed for a test of spatial clustering of waterfalls at distinct profile locations versus a steady increase in waterfall occurrence with distance upstream for streams of different lengths.

3.0 RESULTS

3.1 Waterfall Morphology

I identified 360 waterfalls in the SGM that ranged in height from 1.5 m to 35 m and spacing from 4 m to 7 km (Fig. 6, Table 4). Increasing channel slope resulted in a decrease in waterfall spacing (Fig. 6A) and an increase in waterfall height above S~0.03 (Fig. 6B). Driven primarily by changes in waterfall spacing, the waterfall height to unit length ratio (H_{wf} / L_U) increases with both the waterfall unit slope (S_U) and the river slope (S_R) (Fig. 6C,D). Despite autocorrelation when comparing H_{wf} / L_U with S_U, the position of the data relative to the 1:1 line is insightful, and shows that waterfall height accounts for a larger fraction of relief of the waterfall unit as slope increases (Fig. 6C). Comparing H_{wf} / L_U to the river slope between waterfalls (excluding relief from waterfalls), S_R, (Fig. 6D) removes some of the autocorrelation present in Fig. 6C, resulting in increased scatter, but still shows a statistically significant correlation between waterfall morphology and slope, consistent with cyclic step theory (Izumi et al., 2017). These results showed little

sensitivity to reasonable changes in the threshold values of drainage area, height, and slope used to define waterfalls (Supplemental Material, Figs. S2-4).

3.2 Interpretation of Statistical Analysis

The SGM data, cyclic step experiments, Wohl and Grodek (1994) field survey, and my survey in the Ruby Mountains all show correlations in metrics with channel slope and agree whether positive or negative within scatter. I observed no statistically significant difference in the correlations between waterfall metrics and slope in the Big Tujunga versus Front Range in that their Pearson Correlation Coefficient ρ value is within the same scatter with a 95% confidence range for all the metrics (Fig. 6). The waterfall unit morphology in the SGM is, to first-order, consistent with previous cyclic step experiments and field surveys, which also show a decrease in waterfall spacing with slope and no clear relationship between channel slope and step height for $S < \sim 0.03$ (Fig. 6). The K-S test revealed that there was no statistically significant difference in the distribution of waterfall spacing between the Front Range and Big Tujunga watershed (H=0 for L_U); however, waterfalls in the Big Tujunga tended to be slightly taller than in the Front Range (Fig. 7) (H=1 for H_{wf}). The waterfall spacing also showed a higher correlation between the Front Range and Big Tujunga than waterfall height (P=0.1224 and P=0.0013, respectively) (Fig. 7).

3.3 Waterfall Spatial Distribution

The fraction of the total channel relief from waterfalls increases with increasing channel slope in both the Front Range and Big Tujunga (Fig. 8), with waterfalls first appearing at $\sim 0.03 < S < 0.07$. The fraction of relief from waterfalls in Big Tujunga reaches

slightly higher levels than in the Front Range. Despite consistent waterfall morphology in the Front Range and Big Tujunga (Fig. 6), waterfall spatial distribution differs between these areas. In the Front Range, waterfall frequency increases approaching the channel head, while in the Big Tujunga, waterfall frequency peaks at two distinct non-dimensional distances along the channel (Fig. 9A). In both cases, the spatial distribution of waterfalls follows the trends in channel slope (Fig. 9B,C). The mapped distribution of waterfalls in both the Front Range and Big Tujunga regions shows no qualitative correlation with the location of faults that bisect watersheds and waterfalls exist both upstream and downstream of faults (Fig. 2).

4.0 DISCUSSION

4.1 Comparison with Cyclic Step Experiments and Field Surveys

Differences in the scaling between channel slope, waterfall spacing, and height between the SGM, other field sites, and previous experiments may stem from a variety of factors. The use of Lidar to identify waterfalls in the SGM limits our ability to identify small steps, likely creating a larger waterfall spacing than expected in field surveys. Furthermore, variability in substrate and sediment supply regimes between the SGM, previous bedrock step surveys, and cyclic step experiments can lead to different erosional efficiencies that modulate cyclic step morphology (e.g., Parker and Izumi, 2000; Yokokawa et al., 2013; Izumi et al., 2017). Despite these differences, I interpret the consistent morphologic trends between the SGM, previous field surveys and experiments (Fig. 6) to indicate that SGM waterfalls are predominately autogenic in origin. The Pearson Coefficient statistical analysis not only revealed that the SGM, field survey, and

experimental data all scales with slope, but the correlation between waterfall metrics and slope and similar between these groups (Fig. 6); thus indicating that these cyclic steps and autogenic waterfalls are bedrock bedforms that form with a characteristic morphology under set river slopes despite the variation in other conditions.

4.2 Autogenic Waterfalls as Bedrock Bedforms

The scaling between waterfall morphology and channel slope, as well as the consistency between the SGM, flume experiments, field surveys (Fig. 6), and cyclic step theory are consistent with autogenic waterfall formation. This is further supported by the onset of waterfall occurrence at ~$0.03<S<0.07$ (Fig. 8), matching predictions for the onset of supercritical flow (Palucis and Lamb, 2017) (Fig. 1) and consistent with the idea that supercritical flow drives autogenic waterfall formation (Scheingross et al., 2019). Our results suggest that there may be a threshold slope for autogenic waterfall formation which dictates the bedform morphology, but further research is needed to investigate this in a range of environments and conditions. The consistency of waterfall occurrence with the criteria for autogenic origin and lack of consistency with the criteria for an externally-forced origin make waterfall self-formation the simplest explanation for waterfall occurrence in the SGM.

4.3 Transient Versus Steady State Landscapes

While waterfall formation is often associated with tectonic perturbations, the agreement in waterfall morphology with channel slope between the steady state Front Range region and the transient Big Tujunga (Fig. 6) region suggests that waterfall formation is largely insensitive to the mechanism of relief generation (e.g., sustained

steady uplift or base level perturbation). Instead, the data suggest that the signature of a base-level perturbation is encoded in the position of autogenic waterfalls along the river long profile (Fig. 9) and perhaps in waterfall height (Fig. 7). This is supported by the increase in waterfall frequency with increasing slope towards the channel head in the Front Range, whereas in the Big Tujunga, waterfalls cluster at non-dimensional distances of ~0.3 and 0.7, which have high slopes corresponding with tectonic knickpoints (Fig. 9) (DiBiase et al., 2015). In both cases, waterfall morphology and frequency scale with slope (Fig. 6,9), but waterfall occurrence is dictated by the tectonic forcing in the Big Tujunga. The K-S statistical test (Fig. 7) and the higher fraction of relief from waterfalls in Big Tujunga (Fig. 8) suggest that perhaps waterfalls are taller in transient zones; however, this could also be due to the E-W gradient in relief in the SGM and requires more field tests for verification.

4.4 Implications for Landscape Evolution

As waterfall formation can change erosion rates relative to reaches without waterfalls (Scheingross and Lamb, 2017), autogenic waterfall formation has the potential to modify channel response to perturbations in external forcing, and may even lead to the formation of autogenic knickzones (Scheingross et al., 2020). More research is needed to determine whether autogenic waterfalls can propagate upstream and combine to form knickzones. If this is the case, this could impact how channel morphology is used to interpret Geologic history. Systematic identification of autogenic waterfalls, as presented here, represents a new tool that can be used to analyze landscapes, and determine when

autogenic dynamics may dampen or amplify signals of past climatic and tectonic perturbations.

5.0 CONCLUSION

Waterfalls have the ability to change the erosional regimes of streams and are therefore important for understanding landscape evolution and geologic history encoded in topography. Waterfalls have traditionally been associated with tectonic perturbations, climatic variability, or lithologic heterogeneity; however, it was recently proposed that waterfalls can also form autogenically. The consistent morphologic trends in the SGM and their strong correlation with slope not only suggests that autogenic waterfalls are ubiquitous in nature, but also indicates that they form with a characteristic morphologic signature. The spacing between waterfalls decreases and the step height and height to length ratio of waterfalls both increase with increasing slope. The consistency between the SGM, field surveys, and cyclic step experiments suggests that autogenic waterfalls are bedrock bedforms that form with a characteristic morphology with slope despite variation in substrate, flow regime, channel scale, and more. The onset of autogenic waterfalls at channel slopes of 3-7% is consistent with predictions for Froude supercritical flow and suggests that there may be a threshold slope for autogenic waterfall formation in bedrock. Though the morphology and frequency of waterfalls seems to be dictated by slope rather than the relief generation mechanism, the signal of tectonic forcing is perhaps encoded in the location of waterfalls along the channel. In other words, the relief in the channel can be generated by steady, sustained uplift or tectonic perturbation, but autogenic waterfalls can form wherever the conditions for their

formation are met. This work provides unique criteria to identify autogenic waterfalls in the field, which can function as a new tool to analyze landscapes and determine whether autogenic dynamics may modulate signals of climatic and tectonic perturbations.

REFERENCES CITED

Ashida, K., and Sawai, K., 1977, A study on the stream formation process on a bare slope (3) – three-dimensional channel form: Disaster Prevention Research Institute Annuals: Kyoto University, Japan, v. 20.

Baynes, E.R.C., Lague, D., and Kermarrec, J.-J., 2018b, Supercritical river terraces generated by hydraulic and geomorphic interactions: Geology, v. 46, p. 499–502, doi:10.1130/G40071.1.

Berlin, M.M., and Anderson, R.S., 2007, Modeling of knickpoint retreat on the Roan Plateau, western Colorado: Journal of Geophysical Research: Earth Surface, v. 112, doi:10.1029/2006JF000553.

Berlin, M.M., and Anderson, R.S., 2009, Steepened channels upstream of knickpoints: Controls on relict landscape response: Journal of Geophysical Research: Earth Surface, v. 114, doi:10.1029/2008JF001148.

Brooks, P.C., 2001, Experimental study of erosional cyclic steps [Master's Thesis]: University of Minnesota, 73 p.

Crosby, B.T., and Whipple, K.X., 2006, Knickpoint initiation and distribution within fluvial networks: 236 waterfalls in the Waipaoa River, North Island, New Zealand: Geomorphology, v. 82, p. 16–38, doi:10.1016/j.geomorph.2005.08.023.

DiBiase, R.A., Whipple, K.X., Heimsath, A.M., and Ouimet, W.B., 2010, Landscape form and millennial erosion rates in the San Gabriel Mountains, CA: Earth and Planetary Science Letters, v. 289, p. 134–144, doi:10.1016/j.epsl.2009.10.036.

DiBiase, R.A., Whipple, K.X., Lamb, M.P., and Heimsath, A.M., 2015, The role of waterfalls and knickzones in controlling the style and pace of landscape adjustment in the western San Gabriel Mountains, California: Geological Society of America Bulletin, v. 127, p. 539–559, doi:10.1130/B31113.1.

Duckson, D.W., and Duckson, L.J., 1995, MORPHOLOGY OF BEDROCK STEP POOL SYSTEMS: Journal of the American Water Resources Association, v. 31, p. 43–51, doi:10.1111/j.1752-1688.1995.tb03362.x.

Forte, A.M., Yanites, B.J., and Whipple, K.X., 2016, Complexities of landscape evolution during incision through layered stratigraphy with contrasts in rock strength: Earth Surface Processes and Landforms, v. 41, p. 1736–1757, doi:10.1002/esp.3947.

Frankel, K.L., Pazzaglia, F.J., and Vaughn, J.D., 2007, Knickpoint evolution in a vertically bedded substrate, upstream-dipping terraces, and Atlantic slope bedrock channels: Geological Society of America Bulletin, v. 119, p. 476–486, doi:10.1130/B25965.1.

Grimaud, J.-L., Paola, C., and Voller, V., 2016, Experimental migration of knickpoints: influence of style of base-level fall and bed lithology: Earth Surface Dynamics, v. 4, p. 11–23, doi:10.5194/esurf-4-11-2016.

Izumi, N., Yokokawa, M., and Parker, G., 2017, Incisional cyclic steps of permanent form in mixed bedrock-alluvial rivers: INCISIONAL CYCLIC STEPS: Journal of Geophysical Research: Earth Surface, v. 122, p. 130–152, doi:10.1002/2016JF003847.

Koyama, T., and Ikeda, H., 1998, Effect of riverbed gradient on bedrock channel configuration: A flume experiment: Process Environmental Research Center: Tsukuba University, Japan., no. 23. p. 25-34.

Lavé, J., and Burbank, D., 2004, Denudation processes and rates in the Transverse Ranges, southern California: Erosional response of a transitional landscape to external and anthropogenic forcing: DENUDATION IN THE TRANSVERSE RANGES: Journal of Geophysical Research: Earth Surface, v. 109, doi:10.1029/2003JF000023.

Mackey, B.H., Scheingross, J.S., Lamb, M.P., and Farley, K.A., 2014, Knickpoint formation, rapid propagation, and landscape response following coastal cliff retreat at the last interglacial sea-level highstand: Kaua‘i, Hawai‘i: GSA Bulletin, v. 126, p. 925–942, doi:10.1130/B30930.1.

Malatesta, L.C., and Lamb, M.P., 2018, Formation of waterfalls by intermittent burial of active faults: GSA Bulletin, v. 130, p. 522–536, doi:10.1130/B31743.1.

Neely, A.B., DiBiase, R.A., Corbett, L.B., Bierman, P.R., and Caffee, M.W., 2019a, Bedrock fracture density controls on hillslope erodibility in steep, rocky landscapes with patchy soil cover, southern California, USA: Earth and Planetary Science Letters, v. 522, p. 186–197, doi:10.1016/j.epsl.2019.06.011.

Neely, A.B., and DiBiase, R.A., 2020, Drainage Area, Bedrock Fracture Spacing, and Weathering Controls on Landscape-Scale Patterns in Surface Sediment Grain Size: Journal of Geophysical Research: Earth Surface, v. 125, p. e2020JF005560, doi:10.1029/2020JF005560.

Palucis, M.C., and Lamb, M.P., 2017, What controls channel form in steep mountain streams? Geophysical Research Letters, v. 44, p. 7245–7255, doi:10.1002/2017GL074198.

Scheingross, J.S., and Lamb, M.P., 2017, A Mechanistic Model of Waterfall Plunge Pool Erosion into Bedrock: Journal of Geophysical Research: Earth Surface, v. 122, p. 2079–2104, doi:10.1002/2017JF004195.

Scheingross, J.S., Lamb, M.P., and Fuller, B.M., 2019, Self-formed bedrock waterfalls: Nature, v. 567, p. 229–233, doi:10.1038/s41586-019-0991-z.

Scheingross, J.S., Limaye, A.B., McCoy, S.W., and Whittaker, A.C., 2020, The shaping of erosional landscapes by internal dynamics: Nature Reviews Earth & Environment, v. 1, p. 661–676, doi:10.1038/s43017-020-0096-0.

Schwanghart, W., and Scherler, D., 2014, Short Communication: TopoToolbox 2 – MATLAB-based software for topographic analysis and modeling in Earth surface sciences: Earth Surface Dynamics, v. 2, p. 1–7, doi:10.5194/esurf-2-1-2014.

Sklar, L.S., and Dietrich, W.E., 2001, Sediment and rock strength controls on river incision into bedrock: Geology, v. 29, p. 1087–1090, doi:10.1130/00917613.

Taki, K., and Parker, G., 2005, Transportational cyclic steps created by flow over an erodible bed. Part 1. Experiments: Journal of Hydraulic Research, v. 43, p. 488–501, doi:10.1080/00221680509500147.

Valla, P.G., Beek, P.A. van der, and Lague, D., 2010, Fluvial incision into bedrock: Insights from morphometric analysis and numerical modeling of gorges incising glacial hanging valleys (Western Alps, France): Journal of Geophysical Research: Earth Surface, v. 115, doi:https://doi.org/10.1029/2008JF001079.

Whittaker, A.C., 2012, How do landscapes record tectonics and climate? Lithosphere, v. 4, p. 160–164, doi:10.1130/RF.L003.1.

Whittaker, A.C., and Boulton, S.J., 2012, Tectonic and climatic controls on knickpoint retreat rates and landscape response times: Journal of Geophysical Research: Earth Surface, v. 117, doi:https://doi.org/10.1029/2011JF002157.

Wohl, E.E., and Grodek, T., 1994, Channel bed-steps along Nahal Yael, Negev desert, Israel: Geomorphology, v. 9, p. 117–126, doi:10.1016/0169-555X(94)90070-1.

Wobus, C.W., Crosby, B.T., and Whipple, K.X., 2006, Hanging valleys in fluvial systems: Controls on occurrence and implications for landscape evolution: Journal of Geophysical Research, v. 111, p. F02017, doi:10.1029/2005JF000406.

Yanites, B.J., Tucker, G.E., Mueller, K.J., and Chen, Y.-G., 2010, How rivers react to large earthquakes: Evidence from central Taiwan: Geology, v. 38, p. 639–642, doi:10.1130/G30883.1.

Yokokawa, M., Kotera, A., and Kyogoku, A., 2013, Cyclic steps by bedrock incision: Advances in River Sediment Research, v. 76, p. 629-633, doi:10.14863/geosocabst.2013.0_177.

Yokokawa, M., Izumi, N., Naito, K., Parker, G., Yamada, T., and Greve, R., 2016, Cyclic steps on ice: Journal of Geophysical Research: Earth Surface, v. 121, p. 1023–1048, doi:10.1002/2015JF003736.

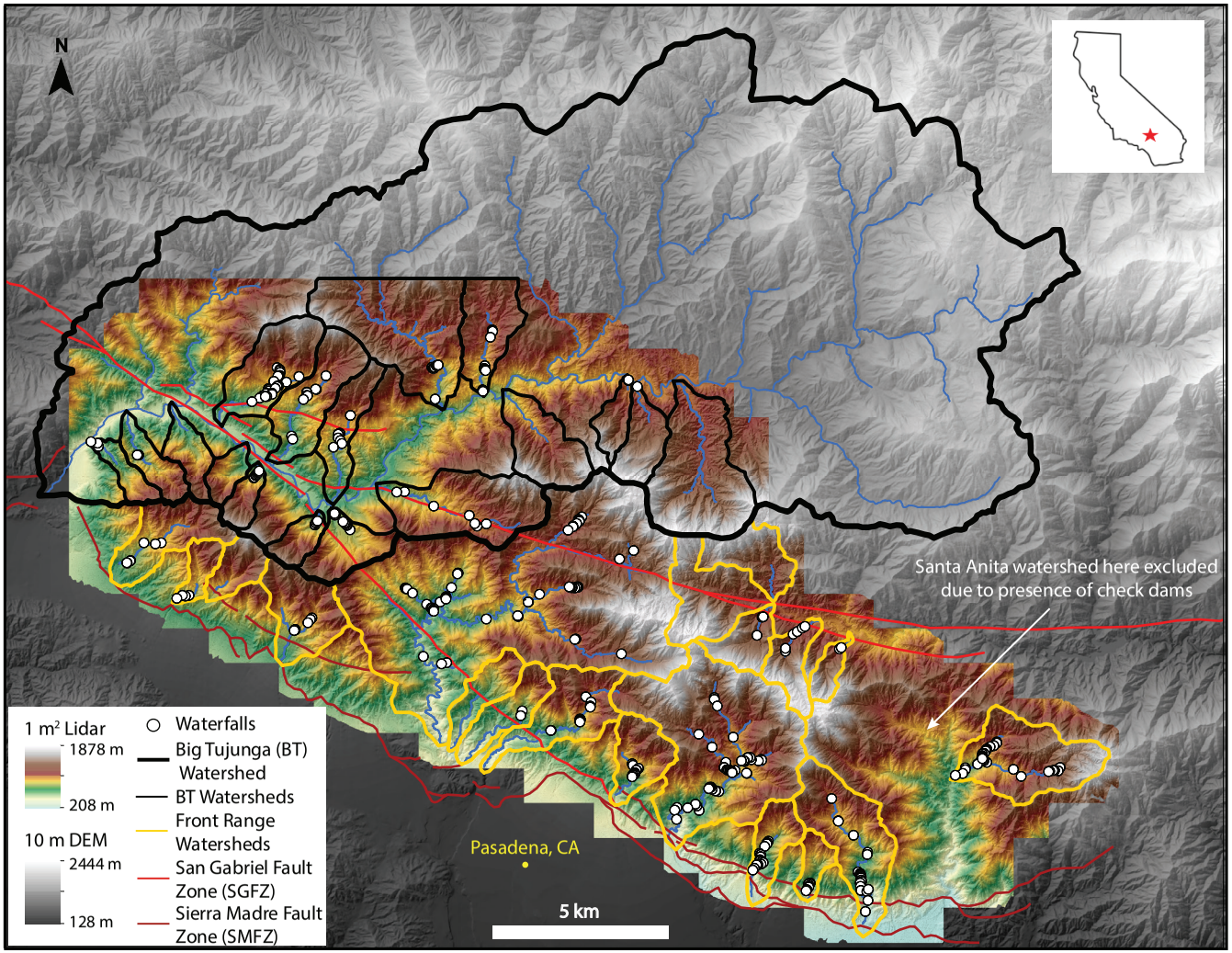

Figure 1: Map of the San Gabriel Mountains, CA showing the Lidar extent and mapped waterfalls in the Front Range and Big Tujunga study areas.

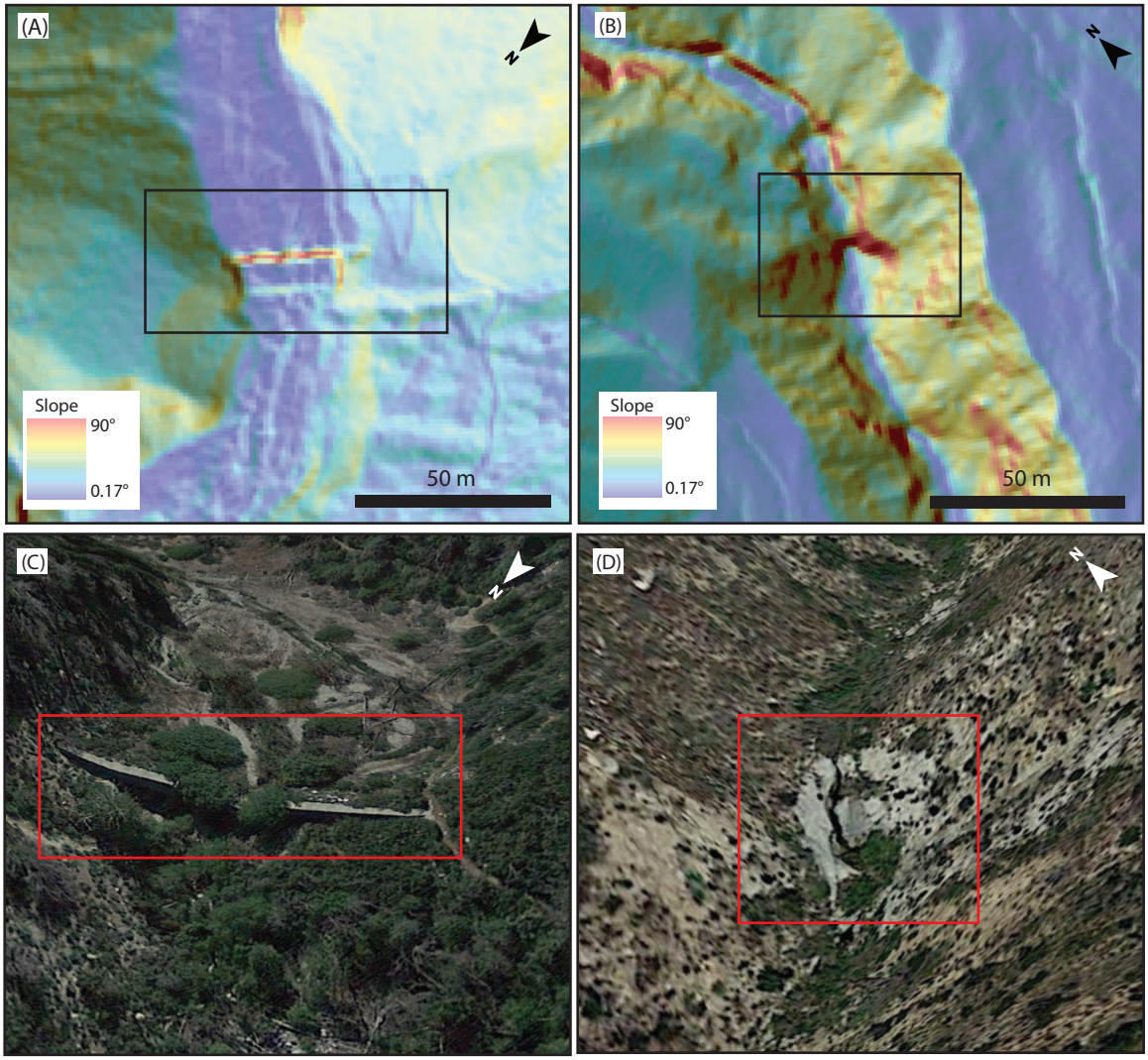

Figure 2: Slopeshade showing check dam on Arroyo Secco (A) and waterfall on Ybarra Canyon (B) in 1m^2 resolution Lidar. (C and D) Google Earth imagery showing visual confirmation of check dam and waterfall from panels (A) and (B), respectively. Length of check dam in panel (C) is 64 m for scale. Width of waterfall in panel (D) is 15 m for scale.

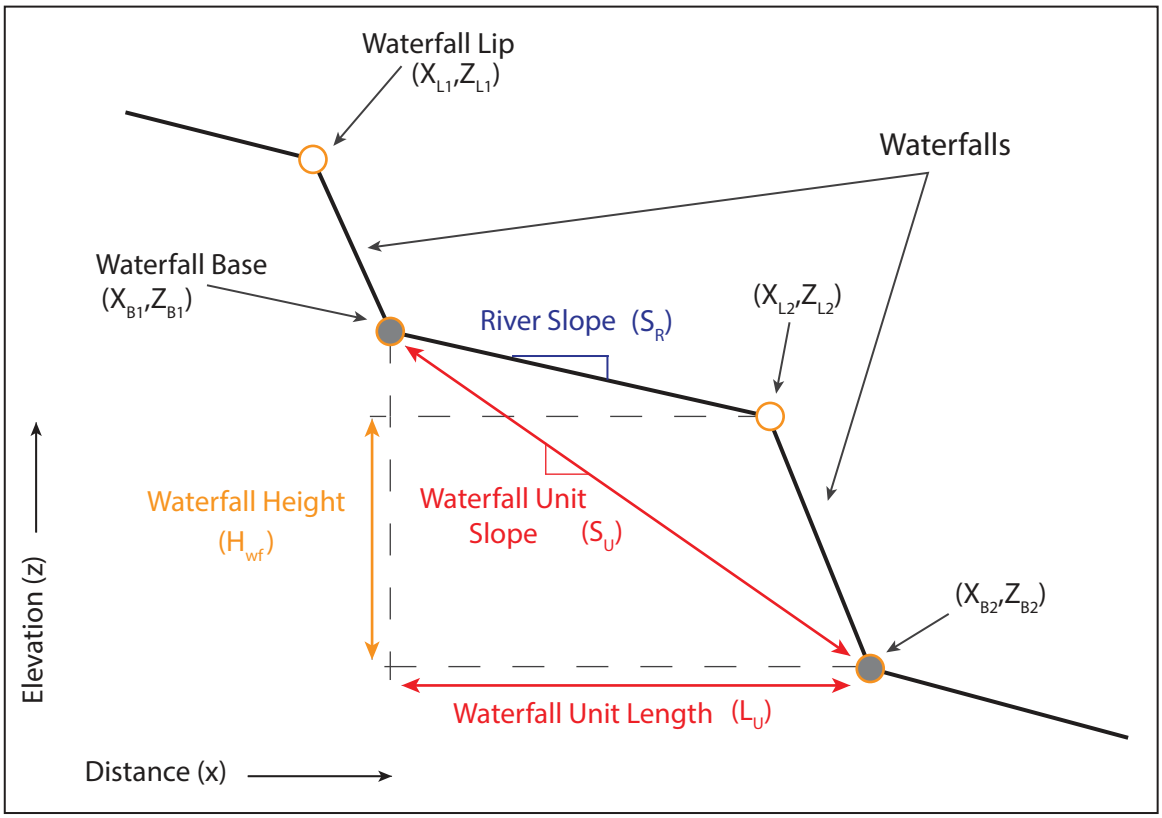

Figure 3: Schematic showing waterfall metrics. A waterfall "unit" was defined from the base of a waterfall (B1) to the base of the next downstream waterfall (B2).

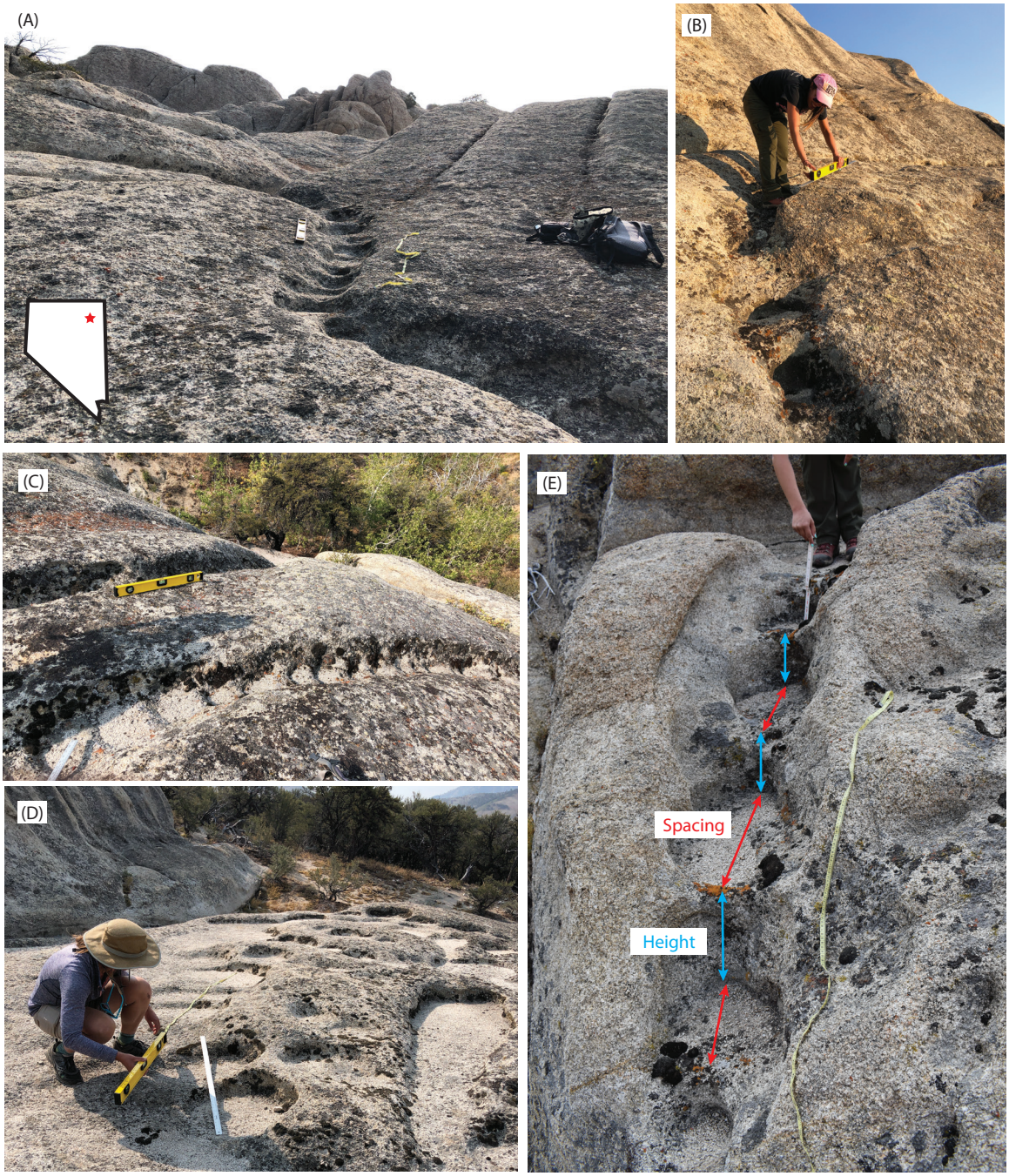

Figure 4: (A-D) Example photos showing cyclic steps formed via overland flow on granitic hillslopes in the Ruby Mountains, NV. Insert in panel (A) shows the location of the Ruby Mountains in Eastern Nevada. (E) Annotated photo defining how step height and spacing were measured for the Ruby Mountains cyclic step survey (See Table 3).

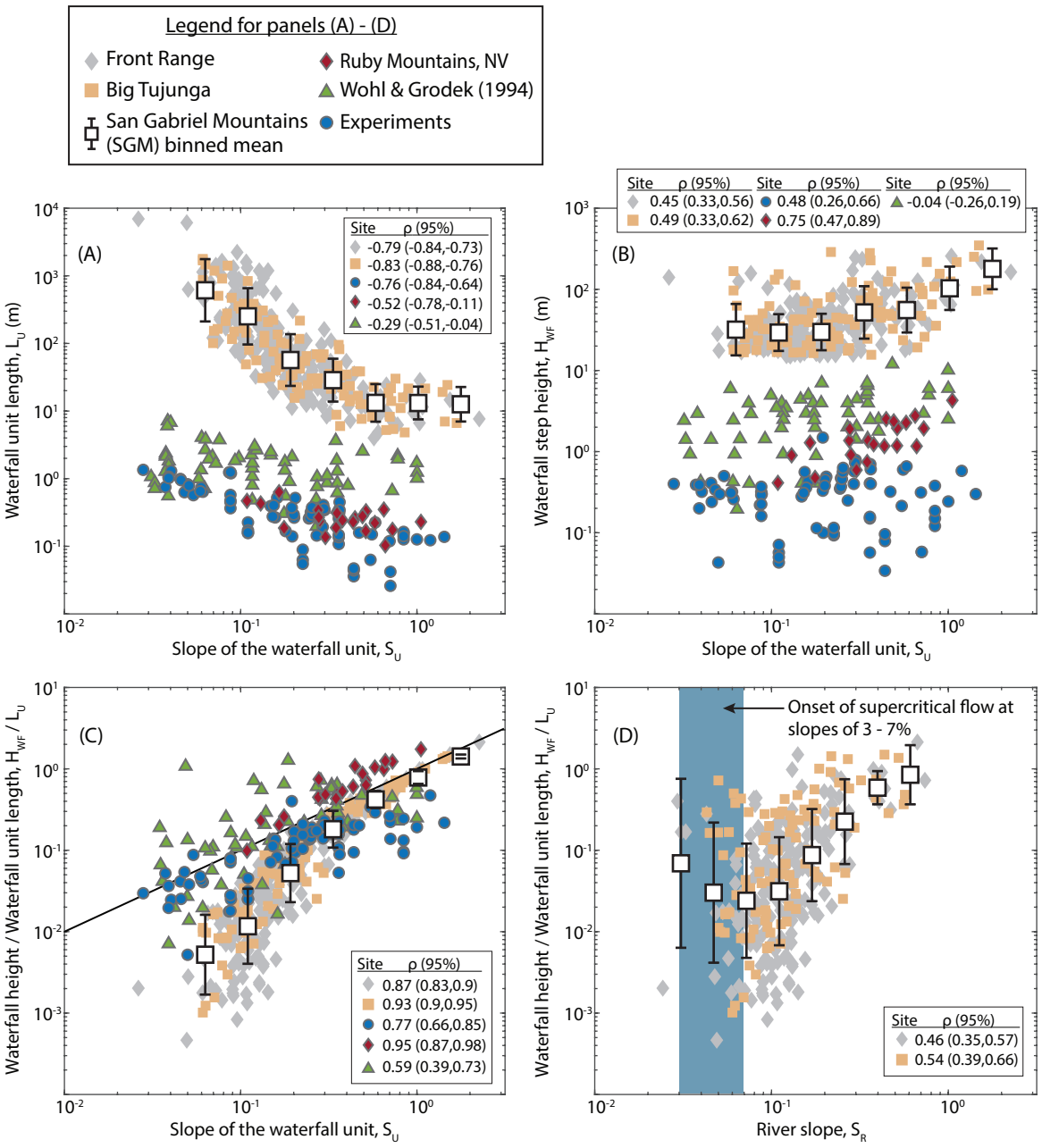

Figure 5: Waterfall unit slope, S_U, versus waterfall length, L_U (A), and waterfall height, H_{wf} (B). H_{wf}/L_U versus the waterfall unit slope, S_U (C) and river slope, S_R (D). Cyclic step experimental data and additional field surveys cannot be plotted in panel (D) due to a lack of data.

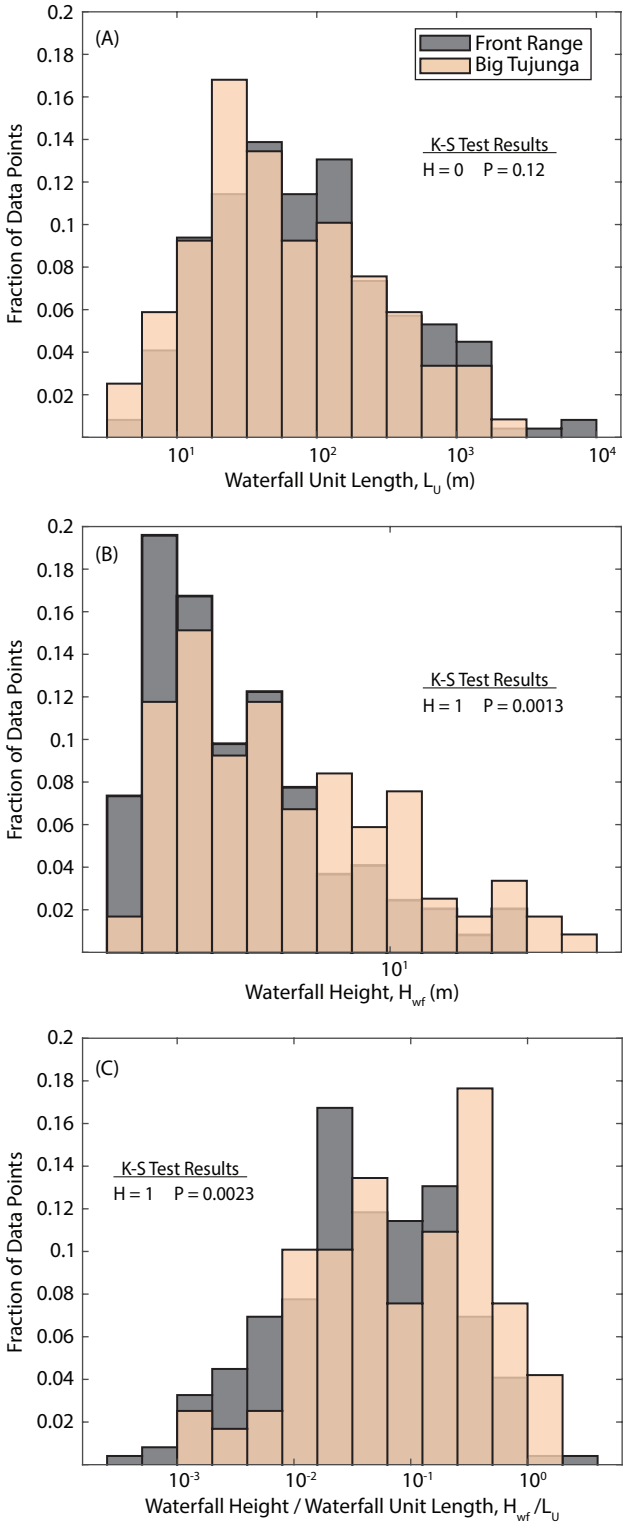

Figure 6: Distribution of waterfall morphology observed in the Front Range and Big Tujunga. (A) Waterfall unit length. (B) Waterfall height. (C) Waterfall height / Waterfall unit length. Kolmogorov-Smirnov (K-S) statistical test results reported where H = 1 indicates the distributions are statistically distinct and H = 0 indicates the data are statistically indistinguishable at the $P < 0.05$ significance level.

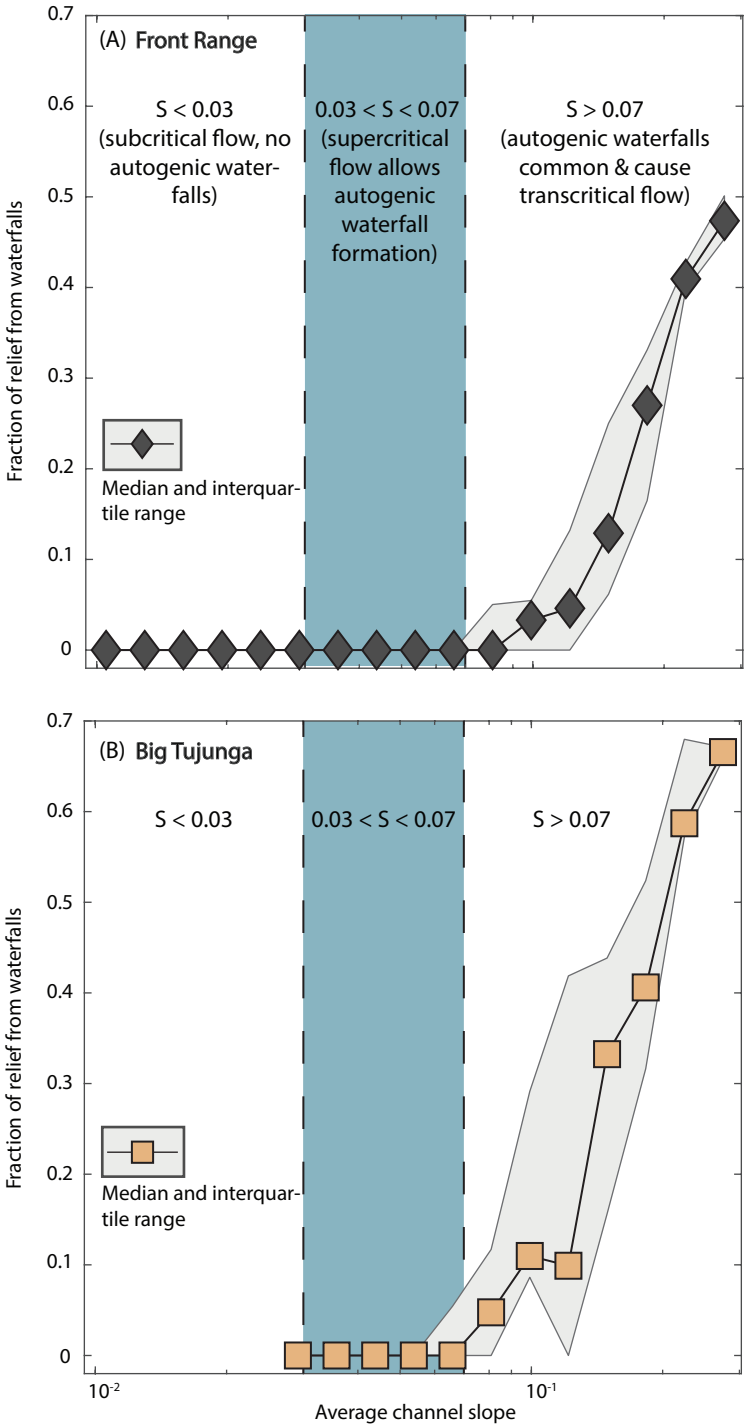

Figure 7: Binned median and interquartile range of the fraction of total channel relief from waterfalls (running average over 500 m) versus the average channel slope (best fit linear regression averaged over 500 m) for the Front Range (A) and Big Tujunga (B).

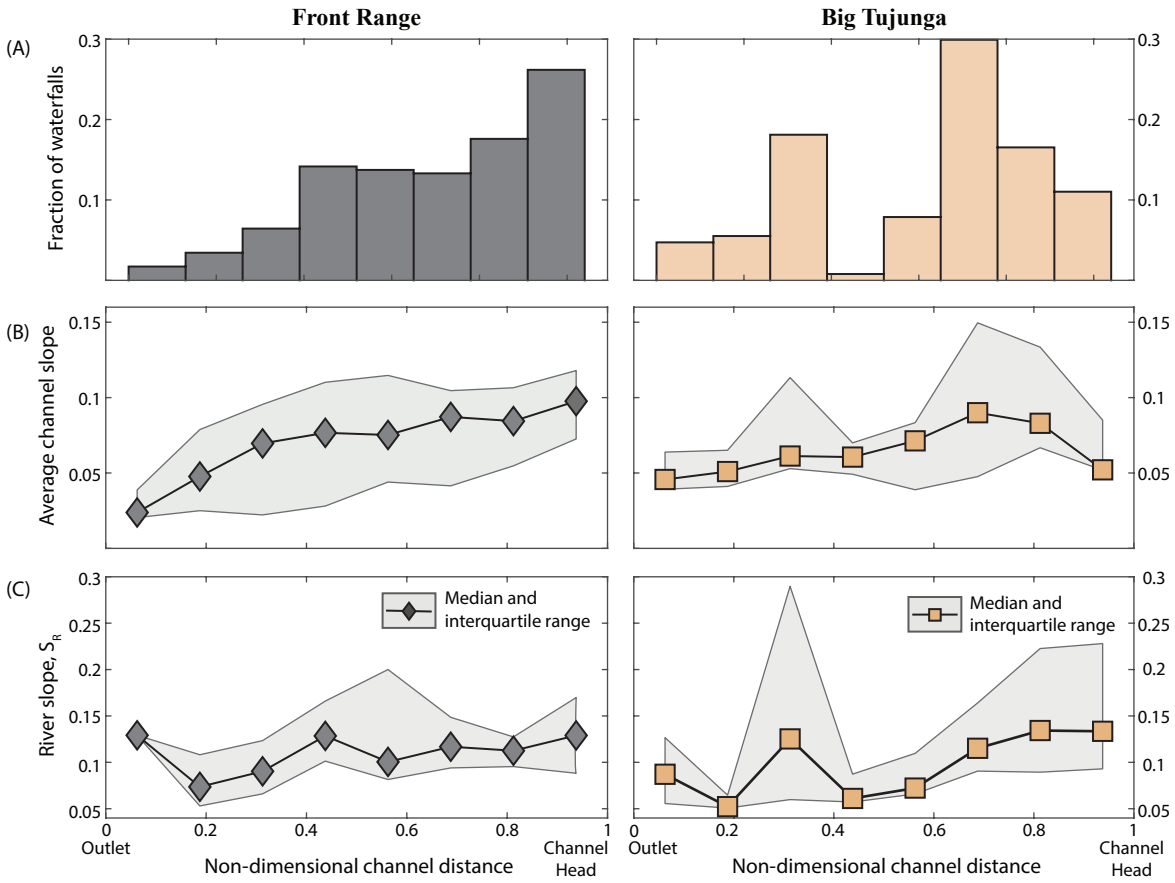

Figure 8: (A) Fraction of waterfalls, (B) channel slope (averaged over 250 m above and 250 m below the waterfall), and (C) channel slope between waterfalls, S_R, versus the non-dimensional distance for the Front Range and Big Tujunga.

TABLE 1. REMOVED CHECK DAMS AND ROADS

Watershed Name	Dam ID	UTM East	UTM North
Arroyo Secco	AS D1	391182.5	3789153.5
Arroyo Secco	AS D2	397158.5	3792298.5
Arroyo Secco	AS D3	397213.5	3792194.5
Arroyo Secco	AS D4	397199.5	3792182.5
Arroyo Secco	AS D5	397125.5	3791788.5
Arroyo Secco	AS D6	396806.5	3791938.5
Arroyo Secco	AS D7	396783.5	3791908.5
Arroyo Secco	AS D8	396631.5	3791837.5
Arroyo Secco	AS D9	396488.5	3791907.5
Arroyo Secco	AS D10	396282.5	3792010.5
Arroyo Secco	AS D11	396055.5	3792030.5
Arroyo Secco	AS D12	395849.5	3792132.5
Arroyo Secco	AS D13	395486.5	3792171.5
Arroyo Secco	AS D14	395286.5	3792264.5
Arroyo Secco	AS D15	394892.5	3792317.5
Arroyo Secco	AS D16	397547.5	3791581.5
Arroyo Secco	AS D17	397419.5	3791611.5
Arroyo Secco	AS D18	397226.5	3791664.5
Arroyo Secco	AS D19	396959.5	3791764.5
Arroyo Secco	AS D20	397091.5	3791463.5
Clear Creek	CL D1	392990.5	3792900.5
Dunsmore Canyon	D D1	385410.5	3791200.5
El Prieto Canyon	EL D1	394009.5	3787600.5
El Prieto Canyon	EL D2	393967.5	3787463.5
El Prieto Canyon	EL D3	393875.5	3787185.5
El Prieto Canyon	EL D4	393765.5	3787230.5
El Prieto Canyon	EL D5	393476.5	3787153.5
El Prieto Canyon	EL D6	393349.5	3787197.5
El Prieto Canyon	EL D7	393236.5	3787107.5
El Prieto Canyon	EL D8	393128.5	3786967.5
El Prieto Canyon	EL D9	392974.5	3786967.5
El Prieto Canyon	EL D10	392862.5	3786775.5
El Prieto Canyon	EL D11	392791.5	3786674.5
El Prieto Canyon	EL D12	392688.5	3786537.5
El Prieto Canyon	EL D13	392530.5	3786379.5
Fern Canyon	FE D1	392816.5	3788072.5
Fern Canyon	FE D2	392693.5	3787993.5
Fern Canyon	FE D3	392118.5	3786723.5
Fern Canyon	FE D4	392107.5	3786726.5
Fern Canyon	FE D5	392088.5	3786625.5
Fern Canyon	FE D6	391955.5	3786514.5
Little Santa Anita Wash	LSA D1	403896.5	3782177.5
Little Santa Anita Wash	LSA D2	403827.5	3781859.5
Millard Creek	M D1	392930.5	3786100.5

Pasadena Canyon	PA D1	400560.5	3782668.5
Pasadena Canyon	PA D2	400558.5	3782656.5
Pasadena Canyon	PA D3	400570.5	3782589.5
Pasadena Canyon	PA D4	400568.5	3782373.5
Sutton Canyon	SU D1	387323.5	3789680.5
Sutton Canyon	SU D2	387293.5	3789513.5
Sutton Canyon	SU D3	387211.5	3789321.5
Sutton Canyon	SU D4	387192.5	3789292.5
Sutton Canyon	SU D5	387142.5	3790518.5
Sutton Canyon	SU D6	387160.5	3790435.5
Sutton Canyon	SU D7	387229.5	3790131.5
Sutton Canyon	SU D8	387323.5	3790011.5

TABLE 2. CYCLIC STEP EXPERIMENTAL DATA

Slope*	L_U** (m)	H_{wf}# (m)	H_{wf} / L_U
Brooks (2001)			
0.16	0.52	0.04	0.08
0.20	0.52	0.05	0.09
0.24	0.26	0.04	0.14
0.29	0.19	0.04	0.21
0.15	0.39	0.03	0.07
0.15	0.40	0.06	0.14
0.16	0.27	0.04	0.13
0.20	0.31	0.03	0.11
0.20	0.27	0.05	0.17
0.25	0.27	0.04	0.14
0.25	0.27	0.05	0.18
0.25	0.32	0.05	0.14
0.29	0.41	0.06	0.14
0.36	0.31	0.07	0.23
0.15	0.28	0.03	0.11
0.20	0.29	0.04	0.13
0.25	0.30	0.06	0.19
0.25	0.37	0.06	0.17
0.30	0.34	0.08	0.23
0.30	0.36	0.07	0.20
Ashida and Sawai (1977)			
0.23	0.09	0.01	0.10
0.23	0.06	0.01	0.15
0.23	0.06	0.01	0.21
0.44	0.04	0.00	0.09
0.44	0.04	0.01	0.18
0.44	0.05	0.01	0.20
0.71	0.04	0.01	0.14
0.71	0.03	0.01	0.22
0.55	0.06	0.02	0.34
0.56	0.15	0.06	0.40
0.20	0.14	0.01	0.07
Koyama and Ikeda (1998)			
0.05	0.83	0.00	0.01
0.11	0.23	0.01	0.03
0.18	0.17	0.01	0.07
0.27	0.14	0.03	0.17
0.36	0.26	0.04	0.16
0.47	0.16	0.03	0.20
0.58	0.23	0.07	0.29
0.70	0.12	0.03	0.26
0.84	0.16	0.04	0.24

1.00	0.13	0.02	0.19
1.19	0.12	0.06	0.47
1.43	0.14	0.03	0.22
0.11	0.17	0.00	0.02
0.36	0.11	0.01	0.05
0.84	0.13	0.01	0.10
0.11	0.16	0.01	0.05
0.36	0.14	0.02	0.11
0.84	0.16	0.02	0.09
0.11	0.16	0.01	0.03
0.36	0.15	0.02	0.11
0.84	0.14	0.02	0.13
Scheingross et al. (2019)			
0.20	0.37	0.15	0.40
Taki and Parker (2005)			
0.04	1.30	0.03	0.02
0.04	0.75	0.04	0.05
0.03	1.35	0.04	0.03
0.04	1.07	0.04	0.04
0.05	0.99	0.04	0.04
0.06	0.64	0.03	0.04
0.05	0.63	0.03	0.05
0.05	0.57	0.05	0.09
0.06	0.74	0.03	0.04
0.05	0.95	0.02	0.03
0.06	0.65	0.03	0.05
0.05	0.79	0.03	0.04
0.04	1.02	0.02	0.02
0.09	1.24	0.02	0.02
0.09	1.20	0.03	0.03
Yokokawa et al. (2016)			
0.09	0.45	0.03	0.07
0.09	0.58	0.02	0.03
0.09	0.37	0.03	0.08
0.36	0.45	0.04	0.09
0.09	1.25	0.02	0.02
0.09	0.47	0.04	0.08
0.36	0.34	0.06	0.18

Note: Each line is a separate experimental run with averaged values for that experiment.

*Slope represents the slope at wich the flume was tilted.

**L_U is the waterfall unit length which was measured from hydraulic jump to hydraulic jump then averaged for each experimental run.

#H_{wf} is the waterfall height averaged for each experimental run.

TABLE 3. FIELD SURVEY FROM RUBY MOUNTAINS, NV CYCLIC STEP METRICS

Survey #	Section #*	Average slope of section** (degrees)	Step #	Pool length# (cm)	Step height (cm)
1	1	27.1	1	22	10
1	1	27.1	2	13.5	15
1	1	27.1	3	20.5	11.5
1	1	27.1	4	20	13.5
1	1	27.1	5	19.5	19
1	1	27.1	6	14.5	10
1	1	27.1	7	15	7
1	1	27.1	8	11.5	10.5
1	1	27.1	9	14.5	10
1	2	15.7	1	16.5	12
1	2	15.7	2	18.5	7
1	2	15.7	3	25.5	10.5
1	2	15.7	4	34	7
1	3	6.2	1	35	5
1	3	6.2	2	39	5.5
1	3	6.2	3	50	4
1	3	6.2	4	64	2
2	1	9.4	1	57.5	15.5
2	1	9.4	2	70	17
2	1	9.4	3	64	6.5
2	1	9.4	4	61	12.5
3	1	36.0	1	25.5	24
3	1	36.0	2	28	12
3	1	36.0	3	12	22
3	1	36.0	4	15	12
3	1	36.0	5	11	17
3	1	36.0	6	8	13
3	1	36.0	7	17	27
3	1	36.0	8	20	23
3	1	36.0	9	21	24
4	1	19.4	1	27	14
4	1	19.4	2	46	15
4	1	19.4	3	19.5	12
4	2	24.0	1	50	42
4	2	24.0	2	15	16.5
4	2	24.0	3	13	17
4	3	46.5	1	21	22.5
4	3	46.5	2	20	26
4	3	46.5	3	28	80
5	1	15.4	1	38	19
5	1	15.4	2	39	16.5
5	1	15.4	3	27	8

5	1	15.4	4	50	11
5	1	15.4	5	17.5	14
5	2	30.0	1	26	17
5	2	30.0	2	22	26
5	2	30.0	3	31	34
5	2	30.0	4	16.5	26.5
5	2	30.0	5	15	10
5	3	33.0	1	37	34
5	3	33.0	2	48	13
5	3	33.0	3	20	36
6	1	27.2	1	22	12
6	1	27.2	2	26	26.5
6	1	27.2	3	51	22
6	1	27.2	4	42	21
6	1	27.2	5	24	16
7	1	33.5	1	14.5	9.5
7	1	33.5	2	8	12.5
7	1	33.5	3	8.5	13
8	1	19.2	1	18	7
8	1	19.2	2	21	5
8	1	19.2	3	14.5	8
8	1	19.2	4	11.5	8
8	1	19.2	5	15	8.5
8	1	19.2	6	30.5	5
8	1	19.2	7	16	6.5
8	1	19.2	8	21	9
8	1	19.2	9	22	10
8	2	15.5	1	27	8.5
8	2	15.5	2	24.5	4
8	2	15.5	3	8.5	9
8	2	15.5	4	12	7
8	2	15.5	5	38	24
8	2	15.5	6	40	14.5
8	2	15.5	7	35	15
8	2	15.5	8	29	70
9	1	16.8	1	24	8.5
9	1	16.8	2	15	7
9	1	16.8	3	7.5	3.5
9	1	16.8	4	8	6.5
9	1	16.8	5	14	5
9	1	16.8	6	13.5	6
9	1	16.8	7	14	5
9	2	10.0	1	15	5
9	2	10.0	2	20	5
9	2	10.0	3	20	2.5
9	2	10.0	4	19.5	6.5
9	3	26.2	1	14	18

9	3	26.2	2	40	35
9	3	26.2	3	41	33
9	3	26.2	4	16.5	8.5
9	4	23.5	1	16	13
9	4	23.5	2	30	4.5
9	4	23.5	3	14	14
9	4	23.5	4	23	18
9	4	23.5	5	32	9
9	5	7.4	1	52	8
9	5	7.4	2	33	17
9	5	7.4	3	38	4.5
9	5	7.4	4	22	5
9	5	7.4	5	70	10.5
9	6	20.7	1	39	17
9	6	20.7	2	24	15.5
9	6	20.7	3	27	14
9	6	20.7	4	28	10.5
9	6	20.7	5	10	6
9	6	20.7	6	18	11

Note: Location of hillslope for surveys is 40.3030726,-115.5089211

*Surveys were split into sections where the slope changed within a group of steps.

**Slope was measured across the length of steps and across the hillslope beside the steps then averaged.

[#]Pool length was used as a proxy for the waterfall unit length and was measured from the base of the upstream step to the lip of the downstream step.

TABLE 4. SAN GABRIEL MOUTAINS, CA WATERFALL METRICS

Watershed Name	Waterfall ID	UTM East	UTM North	X_L*	X_B**	Z_L#	Z_B##	Drainage Area	Non-Dimensional Distance###	S_R*#	S_U**#	L_U+	H_{wf}++
				(m)	(m)	(m)	(m)	(km^2)				(m)	(m)
Arroyo Secco	AS1	396851.5	3789232.5	20909.1	20906.6	1217.8	1216.2	1.7	1.0	N.D.	N.D.	N.D.	N.D.
Arroyo Secco	AS2	395543.5	3789651.5	18682.2	18680.2	1005.6	1003.7	4.4	0.8	0.09	0.10	2226.42	1.86
Arroyo Secco	AS3	395517.5	3789637.5	18637.0	18634.6	998.7	997.1	4.4	0.8	0.12	0.14	45.63	1.60
Arroyo Secco	AS4	392983.5	3790219.5	12533.9	12530.9	698.2	695.3	24.3	0.6	0.05	0.05	6103.69	2.84
Arroyo Secco	AS5	391184.5	3789151.5	5587.0	5580.1	526.8	512.7	36.9	0.3	0.02	0.03	6950.76	14.06
Arroyo Secco	AS6	397195.5	3792182.5	23847.0	23835.0	1250.2	1242.2	1.6	1.0	N.D.	N.D.	N.D.	N.D.
Arroyo Secco	AS7	396800.5	3791932.5	22782.8	22757.4	1175.6	1159.9	1.7	0.9	0.06	0.08	1077.53	15.75
Arroyo Secco	AS8	395719.5	3793147.5	21919.5	21917.5	1182.7	1181.1	1.1	1.0	N.D.	N.D.	N.D.	N.D.
Arroyo Secco	AS9	395623.5	3793073.5	21728.0	21723.6	1163.3	1156.5	1.6	1.0	0.09	0.13	193.95	6.83
Arroyo Secco	AS10	395630.5	3793056.5	21707.3	21704.4	1155.2	1153.5	1.6	1.0	0.08	0.15	19.14	1.64
Arroyo Secco	AS11	395653.5	3793029.5	21665.2	21662.2	1149.1	1146.7	1.6	1.0	0.11	0.16	42.21	2.35
Arroyo Secco	AS12	395645.5	3793018.5	21650.3	21646.5	1143.4	1140.2	1.6	1.0	0.28	0.42	15.73	3.25
Arroyo Secco	AS13	395557.5	3792935.5	21492.7	21490.3	1126.0	1123.9	1.6	1.0	0.09	0.10	156.20	2.08
Arroyo Secco	AS14	395568.5	3792956.5	21464.9	21462.9	1121.9	1119.1	1.6	1.0	0.08	0.18	27.38	2.82
Arroyo Secco	AS15	395460.5	3792878.5	21251.8	21249.4	1100.4	1098.4	1.6	1.0	0.09	0.10	213.55	1.94
Arroyo Secco	AS16	395466.5	3792856.5	21224.5	21222.1	1096.4	1094.5	1.6	1.0	0.08	0.15	27.31	1.90
Arroyo Secco	AS17	395325.5	3792758.5	20961.7	20959.7	1074.7	1072.8	2.6	0.9	0.08	0.08	262.39	1.85
Arroyo Secco	AS18	395614.5	3791137.5	18118.9	18113.9	1129.2	1121.9	1.1	1.0	N.D.	N.D.	N.D.	N.D.
Arroyo Secco	AS19	395606.5	3791145.5	18105.2	18097.4	1120.0	1111.6	1.1	1.0	0.22	0.62	16.49	8.37
Arroyo Secco	AS20	395581.5	3791143.5	18073.2	18069.2	1108.6	1105.0	1.2	1.0	0.13	0.23	28.14	3.53
Arroyo Secco	AS21	395563.5	3791134.5	18050.9	18047.5	1102.6	1099.1	1.2	1.0	0.14	0.27	21.73	3.47
Arroyo Secco	AS22	395519.5	3791114.5	17995.5	17992.5	1090.3	1088.2	1.2	1.0	0.17	0.20	55.04	2.10
Arroyo Secco	AS23	395444.5	3791124.5	17908.9	17905.4	1071.5	1069.0	1.3	1.0	0.20	0.22	87.01	2.54
Arroyo Secco	AS24	395427.5	3791121.5	17888.1	17884.1	1067.1	1063.8	1.3	1.0	0.11	0.24	21.31	3.26
Arroyo Secco	AS25	395391.5	3791125.5	17840.1	17836.7	1055.5	1053.4	1.4	1.0	0.19	0.22	47.46	2.18
Arroyo Secco	AS26	395359.5	3791146.5	17795.9	17792.5	1043.0	1040.1	1.4	1.0	0.25	0.30	44.21	2.83
Arroyo Secco	AS27	394508.5	3790926.5	16601.4	16599.4	871.7	869.5	2.2	0.9	0.14	0.14	1193.07	2.16
Arroyo Secco	AS28	394195.5	3790713.5	16026.1	16023.7	812.0	809.7	2.5	0.9	0.10	0.10	575.74	2.24
Arroyo Secco	AS29	394182.5	3790709.5	16008.6	16006.2	807.6	806.1	2.5	0.9	0.14	0.21	17.49	1.56
Arroyo Secco	AS30	393895.5	3790298.5	15386.6	15379.9	822.5	817.8	1.1	1.0	N.D.	N.D.	N.D.	N.D.
Arroyo Secco	AS31	393885.5	3790305.5	15373.7	15368.9	814.8	811.3	1.1	1.0	0.47	0.58	11.07	3.48
Arroyo Secco	AS32	393887.5	3790315.5	15359.8	15340.5	807.5	781.8	1.1	1.0	0.42	1.04	28.38	25.72
Arroyo Secco	AS33	392176.5	3791536.5	10823.6	10820.6	746.5	743.3	1.0	1.0	N.D.	N.D.	N.D.	N.D.
Arroyo Secco	AS34	392171.5	3791534.5	10817.7	10814.3	742.1	738.5	1.0	1.0	0.42	0.78	6.24	3.65
Arroyo Secco	AS35	392159.5	3791511.5	10787.8	10782.5	735.1	727.6	1.2	1.0	0.13	0.34	31.80	7.45
Arroyo Secco	AS36	391993.5	3791125.5	10250.7	10247.3	678.3	675.8	1.4	0.9	0.09	0.10	535.22	2.50
Arroyo Secco	AS37	391666.5	3790710.5	9446.2	9436.6	609.2	598.8	3.9	0.9	0.08	0.10	810.75	10.44
Arroyo Secco	AS38	390671.5	3791113.5	10315.5	10312.5	740.8	738.4	1.4	1.0	N.D.	N.D.	N.D.	N.D.
Arroyo Secco	AS39	390693.5	3791093.5	10226.5	10224.5	727.1	724.9	1.4	1.0	0.13	0.15	87.91	2.16
Arroyo Secco	AS40	390719.5	3791077.5	10172.6	10169.2	721.7	717.4	1.4	1.0	0.06	0.14	55.36	4.33
Arroyo Secco	AS41	390878.5	3790959.5	9847.4	9843.9	690.5	687.6	1.6	1.0	0.08	0.09	325.25	2.86
Arroyo Secco	AS42	391278.5	3790643.5	9057.4	9055.0	636.1	634.4	1.8	0.9	0.07	0.07	788.92	1.69
Arroyo Secco	AS43	391413.5	3790537.5	8815.3	8812.8	617.9	615.9	1.9	0.9	0.07	0.08	242.18	2.05
Arroyo Secco	AS44	391435.5	3790540.5	8783.0	8780.6	611.8	610.1	1.9	0.8	0.14	0.18	32.21	1.67
Arroyo Secco	AS45	391481.5	3790522.5	8715.9	8713.9	606.1	603.5	1.9	0.8	0.06	0.10	66.70	2.61
Arroyo Secco	AS46	391476.5	3790477.5	8662.5	8658.6	599.5	591.1	1.9	0.8	0.08	0.22	55.28	8.43
Arroyo Secco	AS47	391466.5	3790464.5	8636.7	8634.7	588.4	586.8	1.9	0.8	0.12	0.18	23.90	1.61
Arroyo Secco	AS48	391480.5	3790449.5	8612.4	8608.4	584.5	580.6	1.9	0.8	0.11	0.24	26.31	3.89
Arroyo Secco	AS49	391834.5	3790860.5	9781.1	9778.1	675.5	672.9	1.1	1.0	N.D.	N.D.	N.D.	N.D.
Arroyo Secco	AS50	391834.5	3790853.5	9773.3	9763.4	672.2	650.3	1.1	1.0	0.14	1.54	14.66	21.89
Arroyo Secco	AS51	391832.5	3790831.5	9748.8	9741.4	649.1	639.4	1.1	1.0	0.08	0.50	22.07	9.73
Arroyo Secco	AS52	391831.5	3790797.5	9711.1	9701.6	636.8	629.3	1.1	0.9	0.08	0.26	39.73	7.59
Arroyo Secco	AS53	391853.5	3788973.5	5361.0	5355.2	548.8	543.4	1.3	0.9	N.D.	N.D.	N.D.	N.D.
Arroyo Secco	AS54	391702.5	3788938.5	5140.8	5137.4	526.6	522.9	1.5	0.9	0.08	0.09	217.79	3.69
Bailey Canyon	BA1	402243.5	3782679.5	1120.8	1118.4	513.6	511.5	1.0	1.0	N.D.	N.D.	N.D.	N.D.
Bailey Canyon	BA2	402242.5	3782675.5	1115.6	1106.9	510.4	499.1	1.0	1.0	0.38	1.08	11.49	11.29
Bailey Canyon	BA3	402232.5	3782667.5	1099.7	1095.2	498.5	493.5	1.0	1.0	0.08	0.48	11.66	5.06
Bailey Canyon	BA4	402196.5	3782642.5	1051.5	1047.7	486.7	481.6	1.1	0.9	0.16	0.25	47.53	5.08
Bailey Canyon	BA5	402203.5	3782585.5	978.3	974.9	469.2	465.6	1.1	0.9	0.18	0.22	72.84	3.61
Bailey Canyon	BA6	402208.5	3782561.5	950.6	947.7	462.6	460.7	1.1	0.8	0.12	0.18	27.14	1.96
Bailey Canyon	BA7	402156.5	3782482.5	835.3	831.9	450.9	444.6	1.1	0.7	0.09	0.14	115.81	6.29
Bailey Canyon	BA8	402129.5	3782451.5	790.2	785.4	440.2	431.1	1.1	0.7	0.11	0.29	46.53	9.07
Bryant Canyon	BR1	383047.5	3794910.5	1644.9	1641.1	694.8	692.5	1.3	0.7	N.D.	N.D.	N.D.	N.D.
Bryant Canyon	BR2	383038.5	3794914.5	1634.3	1632.3	691.9	689.4	1.3	0.7	0.09	0.35	8.83	2.46
Bryant Canyon	BR3	383008.5	3794909.5	1601.4	1598.0	686.1	682.6	1.3	0.7	0.11	0.20	34.31	3.42
Clear Creek	CL1	392990.5	3792943.5	5171.1	5165.9	1020.6	1015.9	1.3	1.0	N.D.	N.D.	N.D.	N.D.
Clear Creek	CL2	392722.5	3792876.5	4840.8	4838.4	985.3	983.2	1.4	0.9	0.09	0.10	327.49	2.05
Clear Creek	CL3	392655.5	3792951.5	4696.9	4693.9	970.0	967.7	1.9	0.9	0.09	0.11	144.47	2.35
Clear Creek	CL4	392500.5	3793188.5	4224.3	4220.3	930.6	925.5	2.8	0.8	0.08	0.09	473.62	5.04
Clear Creek	CL5	391482.5	3793448.5	2807.6	2804.2	810.5	806.2	4.9	0.5	0.08	0.08	1416.14	4.21
Clear Creek	CL6	390642.5	3793865.5	1338.0	1335.6	715.2	713.4	7.0	0.2	0.06	0.06	1468.55	1.81
Clear Creek	CL7	390428.5	3793857.5	1061.7	1058.7	692.6	690.2	7.1	0.2	0.08	0.08	276.94	2.35
Coldwater Canyon	COL1	397308.5	3796873.5	265.1	263.1	974.3	972.4	1.9	0.1	N.D.	N.D.	N.D.	N.D.
Cooks Canyon Channel	CO1	384482.5	3790895.5	561.1	558.6	753.0	748.8	1.2	0.5	N.D.	N.D.	N.D.	N.D.

Cooks Canyon Channel	CO2	384383.5	3790873.5	428.5	425.1	735.1	731.0	1.3	0.4	0.10	0.13	133.54	4.15
Cooks Canyon Channel	CO3	384296.5	3790903.5	293.1	290.1	721.1	717.6	1.3	0.2	0.07	0.10	134.95	3.50
Cooks Canyon Channel	CO4	384136.5	3790814.5	66.9	63.9	703.2	700.4	1.4	0.1	0.06	0.08	226.28	2.80
Eaton Wash	EA1	399508.5	3787976.5	10486.2	10483.8	1116.2	1114.2	1.3	0.9	N.D.	N.D.	N.D.	N.D.
Eaton Wash	EA2	399507.5	3787929.5	10430.5	10425.2	1105.7	1100.8	1.6	0.9	0.16	0.23	58.53	4.83
Eaton Wash	EA3	399595.5	3787739.5	10181.7	10179.7	1071.0	1069.3	1.8	0.9	0.12	0.13	245.59	1.72
Eaton Wash	EA4	400050.5	3786843.5	8863.6	8861.6	927.6	925.8	2.5	0.8	0.11	0.11	1318.02	1.75
Eaton Wash	EA5	400101.5	3785894.5	7543.3	7540.9	808.0	805.8	7.4	0.7	0.09	0.09	1320.71	2.16
Eaton Wash	EA6	399632.5	3785291.5	6112.8	6109.4	705.0	702.3	12.5	0.6	0.07	0.07	1431.52	2.72
Eaton Wash	EA7	399543.5	3785314.5	6002.6	5999.8	696.2	694.2	12.6	0.5	0.06	0.07	109.64	1.98
Eaton Wash	EA8	399539.5	3785312.5	5997.8	5995.8	693.7	691.9	12.6	0.5	0.24	0.57	4.00	1.80
Eaton Wash	EA9	399440.5	3785354.5	5829.3	5826.9	680.5	678.0	12.6	0.5	0.07	0.08	168.85	2.53
Eaton Wash	EA10	399406.5	3785421.5	5715.6	5708.8	668.9	661.6	12.7	0.5	0.08	0.14	118.12	7.32
Eaton Wash	EA11	399381.5	3785414.5	5667.3	5664.9	657.4	655.2	12.7	0.5	0.10	0.15	43.87	2.20
Eaton Wash	EA12	399371.5	3785394.5	5640.4	5632.1	653.2	641.2	12.7	0.5	0.08	0.43	32.80	11.96
Eaton Wash	EA13	399346.5	3785377.5	5605.4	5603.4	638.7	637.0	12.7	0.5	0.09	0.15	28.73	1.72
Eaton Wash	EA14	399069.5	3784744.5	4468.2	4465.2	569.8	567.8	14.9	0.4	0.06	0.06	1138.18	2.02
Eaton Wash	EA15	399006.5	3784874.5	4270.4	4268.4	553.9	551.3	14.9	0.4	0.07	0.08	196.79	2.57
Eaton Wash	EA16	398969.5	3784927.5	4192.3	4189.9	546.2	544.0	14.9	0.4	0.07	0.09	78.50	2.21
Eaton Wash	EA17	398747.5	3784823.5	3739.6	3737.6	518.3	516.2	15.1	0.3	0.06	0.06	452.35	2.12
Eaton Wash	EA18	398441.5	3784832.5	3110.9	3108.5	486.2	484.5	15.8	0.3	0.05	0.05	629.07	1.76
Eaton Wash	EA19	398369.5	3784756.5	2940.2	2933.2	473.9	462.3	15.9	0.3	0.06	0.13	175.30	11.57
Eaton Wash	EA20	398425.5	3784496.5	2202.6	2196.2	426.9	414.4	16.2	0.2	0.05	0.07	737.01	12.52
Eaton Wash	EA21	399058.5	3786927.5	9959.8	9956.8	1084.1	1082.1	2.0	0.9	N.D.	N.D.	N.D.	N.D.
Eaton Wash	EA22	399442.5	3786558.5	8960.2	8958.2	994.2	992.2	2.5	0.9	0.09	0.09	998.63	1.95
Eaton Wash	EA23	399831.5	3786130.5	7935.2	7931.2	903.3	899.3	2.8	0.8	0.09	0.09	1026.95	3.92
Eaton Wash	EA24	399779.5	3785979.5	7700.2	7695.8	882.2	877.5	2.9	0.7	0.07	0.09	235.42	4.76
Eaton Wash	EA25	399787.5	3785974.5	7689.0	7686.5	876.3	874.5	2.9	0.7	0.18	0.32	9.24	1.75
Eaton Wash	EA26	399861.5	3785909.5	7561.0	7559.0	857.2	854.8	2.9	0.7	0.14	0.15	127.54	2.37
Eaton Wash	EA27	399886.5	3785903.5	7527.0	7524.6	851.4	849.8	2.9	0.7	0.11	0.15	34.38	1.56
Eaton Wash	EA28	399910.5	3785908.5	7497.1	7494.1	847.0	844.1	2.9	0.7	0.10	0.19	30.56	2.92
Eaton Wash	EA29	399951.5	3785898.5	7447.4	7439.8	836.2	822.5	3.0	0.7	0.17	0.40	54.28	13.71
Eaton Wash	EA30	399981.5	3785879.5	7408.4	7403.6	815.8	809.6	3.0	0.7	0.21	0.36	36.21	6.22
Eaton Wash	EA31	399991.5	3785867.5	7391.7	7387.8	808.2	804.4	3.0	0.7	0.11	0.33	15.73	3.80
Eaton Wash	EA32	400001.5	3785851.5	7368.1	7366.1	802.0	800.3	3.0	0.7	0.12	0.19	21.73	1.71
Eaton Wash	EA33	400007.5	3785841.5	7355.6	7353.6	799.1	797.4	3.0	0.7	0.12	0.24	12.49	1.73
Eaton Wash	EA34	400012.5	3785833.5	7344.4	7342.4	797.1	795.2	3.0	0.7	0.03	0.20	11.24	1.89
Eaton Wash	EA35	400850.5	3786209.5	9148.1	9145.1	1009.5	1007.4	1.6	0.9	N.D.	N.D.	N.D.	N.D.
Eaton Wash	EA36	400866.5	3786188.5	9116.1	9113.7	1002.7	1000.9	1.6	0.9	0.16	0.21	31.38	1.83
Eaton Wash	EA37	400761.5	3786165.5	8798.5	8795.5	965.0	962.4	1.7	0.9	0.11	0.12	318.19	2.64
Eaton Wash	EA38	400562.5	3786202.5	8462.2	8457.2	929.6	924.4	1.7	0.9	0.10	0.11	338.29	5.17
Eaton Wash	EA39	400534.5	3786264.5	8369.2	8367.2	913.1	911.3	1.9	0.9	0.13	0.15	90.01	1.80
Eaton Wash	EA40	400459.5	3786259.5	8264.4	8262.0	899.8	897.9	1.9	0.9	0.11	0.13	105.23	1.92
Eaton Wash	EA41	400458.5	3786251.5	8253.8	8250.3	896.8	893.1	1.9	0.9	0.13	0.41	11.66	3.65
Eaton Wash	EA42	400370.5	3786145.5	8078.5	8075.5	876.8	875.0	1.9	0.8	0.09	0.10	174.82	1.83
Eaton Wash	EA43	400352.5	3786169.5	8042.1	8037.7	871.2	867.2	1.9	0.8	0.11	0.21	37.80	4.06
Eaton Wash	EA44	400337.5	3786181.5	8019.8	8013.4	863.6	850.9	1.9	0.8	0.20	0.67	24.31	12.76
Eaton Wash	EA45	400282.5	3786170.5	7951.3	7949.3	843.7	841.9	1.9	0.8	0.11	0.14	64.11	1.85
Eaton Wash	EA46	400433.5	3785804.5	7808.4	7799.0	854.4	844.3	1.1	1.0	N.D.	N.D.	N.D.	N.D.
Eaton Wash	EA47	400430.5	3785814.5	7796.6	7794.2	843.3	841.4	1.1	1.0	0.41	0.60	4.83	1.93
El Prieto Canyon	EL1	394009.5	3787600.5	3742.5	3738.1	692.9	689.8	1.1	1.0	N.D.	N.D.	N.D.	N.D.
El Prieto Canyon	EL2	393967.5	3787463.5	3582.3	3578.5	669.6	665.7	1.2	0.9	0.13	0.15	159.61	3.83
Fall Creek	F1	393154.5	3798486.5	2663.6	2659.6	1008.8	1003.0	2.1	0.8	N.D.	N.D.	N.D.	N.D.
Fall Creek	F2	393157.5	3798481.5	2656.7	2652.9	1001.7	991.8	2.1	0.8	0.44	1.68	6.66	9.95
Fall Creek	F3	393169.5	3798447.5	2613.0	2605.6	986.1	975.0	2.1	0.8	0.14	0.35	47.28	11.08
Fall Creek	F4	393099.5	3798280.5	2388.3	2385.3	953.6	951.5	2.4	0.7	0.10	0.11	220.31	2.14
Fall Creek	F5	392939.5	3797466.5	1198.7	1196.3	869.0	867.1	3.5	0.3	0.07	0.07	1189.00	1.85
Fall Creek	F6	392921.5	3797386.5	1098.2	1095.3	861.7	860.1	3.5	0.3	0.05	0.07	100.98	1.67
Fall Creek	F7	392935.5	3797372.5	1077.2	1071.8	854.7	850.3	3.5	0.3	0.29	0.42	23.56	4.46
Fall Creek	F8	392948.5	3797349.5	1046.5	1033.2	848.6	831.9	3.5	0.3	0.07	0.48	38.56	16.64
Fall Creek	F9	392953.5	3797333.5	1028.4	1025.0	829.7	827.3	3.5	0.3	0.46	0.55	8.24	2.36
Fall Creek	F10	392959.5	3797327.5	1018.7	1013.9	824.9	818.4	3.5	0.3	0.39	0.81	11.07	6.52
Fall Creek	F11	392881.5	3796773.5	150.8	145.4	775.1	765.4	4.2	0.0	0.05	0.06	868.55	9.68
Fall Creek	F12	392884.5	3796757.5	130.5	122.6	763.4	752.5	4.2	0.0	0.14	0.57	22.73	10.83
Fall Creek	F13	392889.5	3796746.5	114.0	110.0	752.0	745.7	4.2	0.0	0.06	0.54	12.66	6.31
Fall Creek	F14	392894.5	3796727.5	88.7	79.8	744.6	722.9	4.2	0.0	0.05	0.76	30.14	21.71
Falls Canyon	FA1	400724.5	3789761.5	1487.9	1485.5	1214.5	1212.9	1.2	0.9	N.D.	N.D.	N.D.	N.D.
Falls Canyon	FA2	400875.5	3790275.5	820.2	817.7	1129.2	1127.7	1.8	0.5	0.13	0.13	667.78	1.51
Falls Canyon	FA3	400905.5	3790286.5	782.5	773.3	1124.1	1116.4	1.8	0.5	0.10	0.25	44.46	7.78
Fern Canyon	FE1	392574.5	3787922.5	2210.6	2206.6	607.0	604.7	1.7	0.8	N.D.	N.D.	N.D.	N.D.
Fox Creek	FO1	391430.5	3797424.5	2495.4	2493.4	903.5	901.8	8.8	0.3	N.D.	N.D.	N.D.	N.D.
Fox Creek	FO2	391463.5	3797390.5	2438.5	2431.7	896.5	884.2	8.8	0.3	0.10	0.29	61.77	12.28
Fox Creek	FO3	391481.5	3797388.5	2418.0	2416.0	883.6	881.1	8.8	0.3	0.04	0.20	15.66	2.56
Fox Creek	FO4	391495.5	3797398.5	2397.0	2393.5	879.1	872.6	8.8	0.3	0.10	0.38	22.49	6.47
Fox Creek	FO5	391501.5	3797417.5	2374.1	2371.1	871.6	867.9	8.8	0.3	0.05	0.21	22.49	3.71
Fox Creek	FO6	391559.5	3797458.5	2287.3	2275.8	861.7	833.7	8.8	0.3	0.07	0.36	95.23	28.04
Fox Creek	FO7	391579.5	3797472.5	2259.8	2254.5	833.0	826.7	8.8	0.3	0.04	0.33	21.31	6.24
Fox Creek	FO8	391595.5	3797478.5	2239.9	2236.4	825.9	822.9	8.8	0.3	0.06	0.21	18.07	3.02
Fox Creek	FO9	391606.5	3797484.5	2226.4	2221.5	821.3	816.6	8.8	0.3	0.15	0.42	14.90	4.71
Fox Creek	FO10	391611.5	3797487.5	2220.1	2216.7	816.1	812.5	8.8	0.3	0.39	0.85	4.83	3.56

Fox Creek	FO11	391529.5	3796512.5	534.4	527.7	726.3	709.6	10.5	0.1	0.05	0.06	1688.97	16.78
Fusier Canyon	FU1	389098.5	3796049.5	3469.4	3465.9	925.5	922.6	1.2	1.0	N.D.	N.D.	N.D.	N.D.
Fusier Canyon	FU2	389096.5	3796043.5	3461.9	3459.9	922.0	920.4	1.2	1.0	0.16	0.37	6.00	1.56
Fusier Canyon	FU3	388801.5	3795524.5	2555.2	2549.9	852.5	849.0	1.5	0.7	0.08	0.08	909.99	3.49
Fusier Canyon	FU4	388793.5	3795533.5	2542.3	2536.0	848.5	843.2	1.5	0.7	0.06	0.42	13.90	5.29
Fusier Canyon	FU5	388753.5	3795515.5	2468.7	2460.4	838.7	831.6	1.6	0.7	0.07	0.15	75.60	7.13
Fusier Canyon	FU6	388750.5	3795507.5	2459.4	2453.4	831.1	821.5	1.6	0.7	0.52	1.44	7.00	9.55
Fusier Canyon	FU7	388748.5	3795399.5	2307.3	2303.5	811.0	807.8	1.6	0.7	0.07	0.09	149.95	3.22
Fusier Canyon	FU8	388819.5	3795323.5	2142.6	2139.6	798.5	795.6	1.6	0.6	0.06	0.07	163.85	2.84
Fusier Canyon	FU9	388854.5	3795241.5	1988.2	1985.8	787.3	784.8	1.7	0.6	0.06	0.07	153.85	2.51
Fusier Canyon	FU10	388608.5	3795129.5	1343.2	1338.4	749.8	743.6	1.7	0.4	0.05	0.06	647.38	6.29
Grizzly Creek	G1	389088.5	3792773.5	1129.9	1125.7	762.8	759.8	1.3	1.0	N.D.	N.D.	N.D.	N.D.
Grizzly Creek	G2	389009.5	3792895.5	961.7	959.3	744.8	742.5	1.7	0.8	0.09	0.10	166.41	2.30
Grizzly Creek	G3	388994.5	3792909.5	938.6	935.1	739.1	736.7	1.8	0.8	0.16	0.24	24.14	2.44
Grizzly Creek	G4	388964.5	3792938.5	888.1	886.1	733.1	731.4	1.8	0.8	0.08	0.11	49.04	1.69
Grizzly Creek	G5	388948.5	3792948.5	864.8	862.0	728.9	727.2	1.8	0.7	0.12	0.17	24.14	1.64
Grizzly Creek	G6	388936.5	3792970.5	837.8	831.6	723.9	719.6	1.8	0.7	0.14	0.25	30.38	4.35
Grizzly Creek	G7	388886.5	3793002.5	770.0	766.6	706.9	704.2	1.8	0.7	0.21	0.24	65.01	2.68
Grizzly Creek	G8	388666.5	3793194.5	384.7	380.7	661.2	658.5	2.0	0.3	0.11	0.12	385.85	2.75
Grizzly Creek	G9	388653.5	3793200.5	369.2	359.2	654.8	639.2	2.0	0.3	0.32	0.89	21.56	15.58
Grizzly Creek	G10	388650.5	3793239.5	316.9	314.1	633.9	631.7	2.9	0.3	0.13	0.17	45.04	2.17
Grotto Creek	GR1	397047.5	3797035.5	122.6	120.2	952.5	950.4	1.4	0.3	N.D.	N.D.	N.D.	N.D.
Grotto Creek	GR2	397055.5	3797057.5	95.0	85.4	946.1	938.1	1.4	0.2	0.17	0.36	34.80	7.98
Haines Canyon	H1	383686.5	3792400.5	1859.9	1857.1	850.5	846.6	2.3	0.6	N.D.	N.D.	N.D.	N.D.
Haines Canyon	H2	383518.5	3792372.5	1654.0	1650.6	829.3	825.1	2.3	0.5	0.09	0.10	206.51	4.22
Haines Canyon	H3	383195.5	3792398.5	1245.8	1243.8	782.7	780.2	2.5	0.4	0.10	0.11	406.75	2.41
Haines Canyon	H4	382807.5	3791895.5	474.1	472.7	711.3	709.4	3.5	0.1	0.09	0.09	771.16	1.88
Haines Canyon	H5	382803.5	3791885.5	460.8	459.3	708.0	706.0	3.5	0.1	0.12	0.26	13.31	1.96
Haines Canyon	H6	382722.5	3791824.5	340.9	338.5	699.7	697.6	3.6	0.1	0.05	0.07	120.88	2.11
Haines Canyon	H7	382710.5	3791829.5	324.6	322.6	695.8	693.7	3.6	0.1	0.13	0.25	15.90	2.14
Little Santa Anita Wash	LSA1	402857.5	3785087.5	6839.2	6835.4	974.5	972.3	1.1	1.0	N.D.	N.D.	N.D.	N.D.
Little Santa Anita Wash	LSA2	403049.5	3784457.5	5913.2	5909.8	851.5	847.8	1.7	0.9	0.13	0.13	925.57	3.70
Little Santa Anita Wash	LSA3	403049.5	3784446.5	5898.3	5895.9	846.5	844.6	1.7	0.9	0.11	0.23	13.90	1.93
Little Santa Anita Wash	LSA4	403490.5	3784035.5	5118.5	5115.1	766.5	764.3	3.1	0.7	0.10	0.10	780.78	2.16
Little Santa Anita Wash	LSA5	403884.5	3783554.5	4225.6	4221.2	680.7	677.1	4.7	0.6	0.09	0.10	893.96	3.65
Little Santa Anita Wash	LSA6	403881.5	3783492.5	4149.5	4147.1	670.6	668.4	4.8	0.6	0.09	0.12	74.11	2.19
Little Santa Anita Wash	LSA7	403609.5	3782987.5	3126.9	3124.0	577.8	576.0	5.4	0.5	0.09	0.09	1023.02	1.79
Little Santa Anita Wash	LSA8	403679.5	3782945.5	3004.3	2996.9	563.7	556.3	5.5	0.4	0.10	0.15	127.15	7.35
Little Santa Anita Wash	LSA9	403680.5	3782922.5	2974.7	2970.9	552.5	548.2	5.5	0.4	0.17	0.31	25.97	4.31
Little Santa Anita Wash	LSA10	403697.5	3782896.5	2940.3	2938.3	545.7	544.2	5.5	0.4	0.08	0.12	32.63	1.52
Little Santa Anita Wash	LSA11	403698.5	3782882.5	2923.6	2920.2	541.8	538.8	5.5	0.4	0.17	0.30	18.07	3.01
Little Santa Anita Wash	LSA12	403706.5	3782850.5	2887.5	2881.7	535.3	527.2	5.5	0.4	0.11	0.30	38.56	8.10
Little Santa Anita Wash	LSA13	403703.5	3782826.5	2861.4	2857.0	524.0	518.4	5.5	0.4	0.16	0.36	24.66	5.66
Little Santa Anita Wash	LSA14	403709.5	3782757.5	2780.2	2777.8	507.5	505.7	5.6	0.4	0.14	0.16	79.18	1.79
Little Santa Anita Wash	LSA15	403721.5	3782715.5	2730.0	2724.1	499.6	494.2	5.6	0.4	0.13	0.21	53.70	5.43
Little Santa Anita Wash	LSA16	403675.5	3782677.5	2660.7	2656.7	484.7	480.6	5.6	0.4	0.15	0.20	67.43	4.06
Little Santa Anita Wash	LSA17	403690.5	3782584.5	2542.7	2539.9	463.6	461.7	5.7	0.4	0.15	0.16	116.81	1.92
Little Santa Anita Wash	LSA18	403700.5	3782459.5	2357.4	2354.0	442.1	437.6	5.7	0.3	0.11	0.13	185.89	4.54
Little Santa Anita Wash	LSA19	403870.5	3782431.5	1938.2	1936.2	394.1	391.3	5.8	0.3	0.10	0.11	417.79	2.85
Little Santa Anita Wash	LSA20	403907.5	3782490.5	1860.7	1854.9	384.4	379.3	5.8	0.3	0.09	0.15	81.33	5.10
Little Santa Anita Wash	LSA21	403896.5	3782176.5	1369.7	1365.7	340.2	336.1	6.4	0.2	0.08	0.09	489.19	4.12
Lukens Canyon	L1	386340.5	3794259.5	750.3	732.5	770.1	746.7	1.1	1.0	N.D.	N.D.	N.D.	N.D.
Lukens Canyon	L2	386346.5	3794281.5	725.2	718.8	745.2	732.7	1.1	0.9	0.22	1.03	13.66	12.50
Lukens Canyon	L3	386385.5	3794324.5	654.4	649.6	715.9	712.2	1.1	0.8	0.26	0.30	69.18	3.65
Lukens Canyon	L4	386389.5	3794330.5	646.8	644.4	710.6	708.7	1.1	0.8	0.56	0.67	5.24	1.92
Lukens Canyon	L5	386400.5	3794340.5	629.3	622.6	702.8	693.2	1.1	0.8	0.39	0.71	21.73	9.61
Lukens Canyon	L6	386436.5	3794371.5	573.2	568.9	684.6	681.6	1.1	0.7	0.17	0.22	53.70	2.94
Lukens Canyon	L7	386450.5	3794398.5	540.4	530.3	676.5	664.0	1.1	0.7	0.18	0.46	38.63	12.47
Lukens Canyon	L8	386462.5	3794415.5	517.8	513.4	661.2	656.2	1.2	0.7	0.23	0.46	16.90	4.99
Lukens Canyon	L9	386469.5	3794429.5	500.9	496.5	654.8	649.7	1.2	0.6	0.12	0.39	16.90	5.08
Lukens Canyon	L10	386476.5	3794440.5	486.4	480.6	647.3	636.5	1.2	0.6	0.24	0.83	15.90	10.81
Lukens Canyon	L11	386483.5	3794456.5	466.7	461.9	634.0	623.6	1.2	0.6	0.17	0.69	18.73	10.48
Millard Creek	M1	395836.5	3787997.5	6630.7	6628.7	948.5	946.7	2.7	0.8	N.D.	N.D.	N.D.	N.D.
Millard Creek	M2	395980.5	3787850.5	6340.2	6337.8	917.5	915.4	2.8	0.8	0.10	0.11	290.88	2.15
Millard Creek	M3	395961.5	3787734.5	6137.6	6134.6	889.2	886.5	2.8	0.8	0.13	0.14	203.17	2.79
Millard Creek	M4	395963.5	3787701.5	6097.7	6094.8	882.6	880.8	3.0	0.8	0.11	0.14	39.80	1.75
Millard Creek	M5	395659.5	3787359.5	5491.3	5488.3	801.7	799.5	3.4	0.7	0.13	0.13	606.51	2.27
Millard Creek	M6	395669.5	3787352.5	5475.2	5473.2	797.6	796.0	3.4	0.7	0.15	0.23	15.07	1.56
Millard Creek	M7	395671.5	3787338.5	5458.8	5455.3	795.6	792.6	3.4	0.7	0.03	0.19	17.90	3.00
Millard Creek	M8	395665.5	3787313.5	5429.0	5425.0	789.9	786.4	3.4	0.7	0.10	0.20	30.31	3.49
Millard Creek	M9	395661.5	3787286.5	5397.9	5394.9	778.9	776.9	3.5	0.7	0.28	0.32	30.14	2.01
Millard Creek	M10	395664.5	3787280.5	5390.1	5387.6	775.9	773.9	3.5	0.7	0.20	0.42	7.24	2.07
Millard Creek	M11	394834.5	3787038.5	3745.1	3742.7	647.5	645.1	5.1	0.5	0.08	0.08	1644.97	2.37
Millard Creek	M12	394831.5	3787036.5	3741.3	3735.0	644.1	627.8	5.1	0.5	0.67	2.26	7.66	16.34
Pasadena Canyon	PA1	401055.5	3783873.5	2803.9	2801.9	683.1	681.0	1.4	0.9	N.D.	N.D.	N.D.	N.D.
Pasadena Canyon	PA2	401019.5	3783823.5	2726.7	2721.5	673.7	668.9	1.4	0.9	0.10	0.15	80.40	4.83
Pasadena Canyon	PA3	401011.5	3783814.5	2713.8	2704.8	667.0	654.4	1.4	0.9	0.25	0.87	16.66	12.62
Pasadena Canyon	PA4	401012.5	3783800.5	2699.4	2696.4	654.1	651.8	1.4	0.8	0.04	0.31	8.41	2.36
Pasadena Canyon	PA5	401010.5	3783793.5	2691.6	2686.6	651.1	645.2	1.4	0.8	0.15	0.67	9.83	5.88
Pasadena Canyon	PA6	400946.5	3783723.5	2580.5	2578.5	635.6	633.2	1.5	0.8	0.09	0.11	108.05	2.42

Pasadena Canyon	PA7	400799.5	3783519.5	2263.6	2261.6	594.9	593.3	1.7	0.7	0.12	0.13	316.89	1.58
Pasadena Canyon	PA8	400832.5	3783486.5	2211.7	2207.3	588.5	583.1	1.7	0.7	0.10	0.19	54.36	5.35
Pasadena Canyon	PA9	400825.5	3783425.5	2059.9	2057.1	569.3	566.8	1.7	0.6	0.09	0.11	150.20	2.48
Pasadena Canyon	PA10	400826.5	3783421.5	2054.7	2049.4	565.8	561.4	1.8	0.6	0.44	0.71	7.66	4.38
Pasadena Canyon	PA11	400806.5	3783340.5	1953.1	1950.7	553.5	551.2	1.8	0.6	0.08	0.10	98.74	2.27
Pasadena Canyon	PA12	400814.5	3783312.5	1919.0	1914.7	548.1	544.5	1.8	0.6	0.10	0.19	35.97	3.59
Pasadena Canyon	PA13	400876.5	3783292.5	1832.0	1829.0	536.3	533.8	1.8	0.6	0.10	0.12	85.77	2.53
Pasadena Canyon	PA14	400898.5	3783253.5	1775.5	1772.5	528.8	524.9	1.9	0.6	0.09	0.16	56.46	3.96
Pasadena Canyon	PA15	400844.5	3783217.5	1682.0	1679.6	517.5	515.4	2.0	0.5	0.08	0.10	92.91	2.10
Pasadena Canyon	PA16	400759.5	3783193.5	1558.0	1554.6	506.6	501.6	2.0	0.5	0.07	0.11	124.95	5.02
Pasadena Canyon	PA17	400734.5	3783190.5	1525.9	1522.5	499.1	493.8	2.0	0.5	0.09	0.24	32.14	5.23
Pasadena Canyon	PA18	400712.5	3783190.5	1496.7	1494.3	488.4	485.5	2.0	0.5	0.21	0.30	28.21	2.91
Pasadena Canyon	PA19	400646.5	3783095.5	1353.9	1351.5	464.3	462.2	2.0	0.4	0.15	0.16	142.78	2.15
Pasadena Canyon	PA20	400605.5	3783040.5	1264.8	1258.5	448.0	442.1	2.0	0.4	0.16	0.22	92.98	5.85
Pasadena Canyon	PA21	400567.5	3782372.5	462.0	459.6	380.0	378.4	2.2	0.1	0.08	0.08	798.90	1.65
Pipe Canyon	P1	381889.5	3795154.5	471.2	468.8	529.2	527.3	1.4	0.3	N.D.	N.D.	N.D.	N.D.
Pipe Canyon	P2	381886.5	3795159.5	464.9	460.5	526.2	521.5	1.4	0.3	0.28	0.70	8.24	4.73
Pipe Canyon	P3	381875.5	3795246.5	258.7	253.5	496.2	491.9	1.4	0.2	0.13	0.14	207.04	4.28
Pipe Canyon	P4	381675.5	3795288.5	6.2	2.4	464.0	460.9	1.5	0.0	0.11	0.12	251.08	3.10
Rubio Canyon	R1	397160.5	3786080.5	1743.8	1741.8	798.6	796.8	1.3	0.7	N.D.	N.D.	N.D.	N.D.
Rubio Canyon	R2	397176.5	3786037.5	1691.7	1688.7	792.5	789.5	1.3	0.7	0.09	0.14	53.11	3.07
Rubio Canyon	R3	397332.5	3785955.5	1446.2	1441.8	757.6	753.3	1.4	0.6	0.13	0.15	246.89	4.35
Rubio Canyon	R4	397280.5	3785907.5	1354.7	1352.3	741.2	738.8	2.2	0.6	0.14	0.16	89.50	2.41
Rubio Canyon	R5	397273.5	3785899.5	1342.6	1340.2	736.9	735.3	2.2	0.6	0.20	0.29	12.07	1.58
Rubio Canyon	R6	397230.5	3785830.5	1242.5	1231.3	723.3	699.8	2.3	0.5	0.12	0.33	108.91	23.47
Rubio Canyon	R7	397226.5	3785810.5	1220.0	1214.6	699.5	692.8	2.3	0.5	0.03	0.42	16.66	6.67
Rubio Canyon	R8	397225.5	3785790.5	1195.7	1192.3	689.0	685.2	2.3	0.5	0.20	0.34	22.31	3.78
Rubio Canyon	R9	397179.5	3785776.5	1128.1	1123.3	676.5	671.6	2.3	0.5	0.14	0.20	69.01	4.89
Rubio Canyon	R10	397173.5	3785770.5	1117.9	1113.9	670.4	662.6	2.3	0.5	0.23	0.96	9.41	7.77
Rubio Canyon	R11	397152.5	3785726.5	1063.2	1059.2	653.3	644.9	2.3	0.5	0.18	0.32	54.70	8.34
Rubio Canyon	R12	397151.5	3785716.5	1051.4	1047.4	643.2	638.9	2.3	0.5	0.22	0.51	11.83	4.31
Rush Creek	RU1	403087.5	3789368.5	911.5	905.5	1063.9	1057.6	1.0	1.0	N.D.	N.D.	N.D.	N.D.
Rush Creek	RU2	403134.5	3789405.5	828.2	810.1	1047.2	1030.2	1.0	0.9	0.13	0.29	95.43	17.06
Santa Anita Wash	SA1	409398.5	3785977.5	4797.6	4794.2	1229.1	1226.4	1.0	1.0	N.D.	N.D.	N.D.	N.D.
Santa Anita Wash	SA2	409344.5	3785882.5	4658.7	4655.7	1204.0	1201.6	1.3	1.0	0.17	0.18	138.47	2.37
Santa Anita Wash	SA3	409231.5	3785895.5	4519.1	4516.1	1176.3	1173.6	1.3	0.9	0.19	0.20	139.64	2.67
Santa Anita Wash	SA4	409188.5	3785896.5	4469.9	4467.9	1164.3	1162.8	1.6	0.9	0.20	0.22	48.21	1.51
Santa Anita Wash	SA5	409096.5	3785870.5	4357.3	4351.0	1148.7	1141.9	1.6	0.9	0.13	0.18	116.81	6.82
Santa Anita Wash	SA6	409067.5	3785859.5	4323.1	4320.1	1139.5	1137.1	1.6	0.9	0.09	0.16	30.90	2.46
Santa Anita Wash	SA7	408286.5	3785723.5	3167.0	3163.6	993.6	990.6	3.0	0.7	0.12	0.13	1156.51	3.00
Santa Anita Wash	SA8	408062.5	3785921.5	2626.1	2623.1	927.2	924.8	3.3	0.5	0.12	0.12	540.53	2.31
Santa Anita Wash	SA9	407298.5	3786129.5	1565.5	1562.1	821.2	818.2	4.2	0.3	0.10	0.10	1061.03	3.03
Santa Anita Wash	SA10	407217.5	3786171.5	1458.0	1454.2	801.6	798.9	4.2	0.3	0.16	0.18	107.88	2.71
Santa Anita Wash	SA11	407199.5	3786205.5	1416.0	1402.1	795.0	770.5	4.2	0.3	0.10	0.55	52.11	24.53
Santa Anita Wash	SA12	407107.5	3786144.5	1274.4	1271.4	760.2	758.1	6.3	0.3	0.08	0.09	130.71	2.14
Santa Anita Wash	SA13	407046.5	3786088.5	1177.9	1175.5	743.8	742.3	6.4	0.2	0.15	0.16	95.91	1.54
Santa Anita Wash	SA14	407032.5	3786077.5	1156.1	1151.9	738.8	733.0	6.4	0.2	0.18	0.39	23.56	5.78
Santa Anita Wash	SA15	406686.5	3785962.5	630.3	625.5	678.1	674.1	6.8	0.1	0.11	0.11	526.45	3.99
Santa Anita Wash	SA16	406683.5	3785914.5	568.5	564.7	671.4	668.8	6.9	0.1	0.05	0.09	60.77	2.61
Santa Anita Wash	SA17	406610.5	3785812.5	395.1	389.4	644.1	640.2	6.9	0.1	0.15	0.16	175.24	3.88
Santa Anita Wash	SA18	406397.5	3785753.5	91.4	87.4	613.2	610.1	7.0	0.0	0.09	0.10	302.05	3.19
Santa Anita Wash	SA19	407583.5	3786708.5	2352.7	2350.7	976.1	974.3	1.4	0.9	N.D.	N.D.	N.D.	N.D.
Santa Anita Wash	SA20	407579.5	3786673.5	2311.3	2308.4	971.8	969.9	1.4	0.8	0.06	0.10	42.21	1.82
Santa Anita Wash	SA21	407503.5	3786605.5	2162.8	2158.6	951.4	948.8	1.8	0.8	0.13	0.14	149.88	2.62
Santa Anita Wash	SA22	407493.5	3786599.5	2150.3	2147.9	947.3	945.3	1.8	0.8	0.18	0.33	10.66	2.07
Santa Anita Wash	SA23	407393.5	3786574.5	1987.6	1979.4	926.3	917.6	1.8	0.7	0.12	0.16	168.51	8.62
Santa Anita Wash	SA24	407292.5	3786505.5	1827.0	1824.0	899.8	895.5	1.9	0.7	0.12	0.14	155.37	4.34
Santa Anita Wash	SA25	407274.5	3786473.5	1783.2	1780.4	888.1	886.3	1.9	0.6	0.18	0.21	43.63	1.77
Santa Anita Wash	SA26	407266.5	3786461.5	1767.3	1763.9	886.3	881.8	1.9	0.6	0.00	0.28	16.49	4.55
Santa Anita Wash	SA27	407263.5	3786456.5	1761.1	1757.3	881.4	874.9	1.9	0.6	0.13	1.03	6.66	6.51
Santa Anita Wash	SA28	407222.5	3786376.5	1644.0	1641.6	855.8	853.3	1.9	0.6	0.17	0.19	115.67	2.47
Santa Anita Wash	SA29	407173.5	3786370.5	1587.2	1579.2	847.3	837.5	1.9	0.6	0.11	0.25	62.38	9.81
Santa Anita Wash	SA30	407158.5	3786318.5	1515.9	1511.1	827.4	823.6	2.0	0.6	0.16	0.20	68.11	3.71
Santa Anita Wash	SA31	407175.5	3786284.5	1471.7	1465.7	814.7	809.4	2.1	0.5	0.23	0.31	45.38	5.32
Santa Anita Wash	SA32	407170.5	3786260.5	1445.0	1441.6	805.2	801.0	2.1	0.5	0.20	0.35	24.07	4.21
Santa Anita Wash	SA33	407166.5	3786233.5	1413.9	1391.2	795.6	770.7	2.1	0.5	0.19	0.60	50.46	24.95
Silver Creek	SL1	388081.5	3792912.5	942.8	940.8	737.2	735.6	1.2	1.0	N.D.	N.D.	N.D.	N.D.
Silver Creek	SL2	388084.5	3792918.5	935.6	926.7	734.2	725.5	1.2	1.0	0.26	0.72	14.07	8.69
Silver Creek	SL3	388103.5	3792970.5	859.8	857.4	708.5	706.8	1.2	0.9	0.25	0.27	69.36	1.75
Silver Creek	SL4	388114.5	3792976.5	844.9	835.8	704.4	682.8	1.2	0.9	0.19	1.11	21.56	21.69
Silver Creek	SL5	388149.5	3793018.5	784.3	780.9	674.5	670.0	1.2	0.8	0.16	0.23	54.94	4.49
Silver Creek	SL6	388156.5	3793023.5	775.2	761.7	668.5	643.2	1.2	0.8	0.27	1.40	19.14	25.22
Strayns Canyon	ST1	401538.5	3789299.5	1957.6	1954.2	1209.2	1206.4	1.2	0.9	N.D.	N.D.	N.D.	N.D.
Strayns Canyon	ST2	401542.5	3789382.5	1867.2	1864.7	1191.2	1189.7	1.2	0.9	0.17	0.19	89.46	1.55
Strayns Canyon	ST3	401761.5	3789793.5	1317.3	1313.9	1104.8	1102.3	1.4	0.6	0.15	0.16	550.81	2.52
Strayns Canyon	ST4	401873.5	3789857.5	1133.8	1131.4	1079.0	1077.3	1.9	0.5	0.13	0.14	182.58	1.73
Strayns Canyon	ST5	402024.5	3789972.5	917.3	915.3	1049.6	1048.0	2.2	0.4	0.13	0.14	216.04	1.59
Strayns Canyon	ST6	402096.5	3790009.5	813.3	811.3	1035.5	1033.9	2.2	0.4	0.12	0.14	104.05	1.61
Sutton Canyon	SU1	388003.5	3790258.5	2374.4	2372.0	876.2	874.1	1.0	0.9	N.D.	N.D.	N.D.	N.D.
Sutton Canyon	SU2	387960.5	3790209.5	2301.7	2298.9	863.2	861.4	1.1	0.9	0.15	0.17	73.08	1.80

Sutton Canyon	SU3	387886.5	3790117.5	2160.5	2157.1	843.4	840.2	1.2	0.9	0.13	0.15	141.78	3.22
Sutton Canyon	SU4	387520.5	3789925.5	1517.0	1514.0	764.8	761.8	1.4	0.6	0.12	0.12	643.16	3.04
Sutton Canyon	SU5	387521.5	3789919.5	1510.6	1505.7	760.5	756.8	1.4	0.6	0.38	0.60	8.24	3.64
Sutton Canyon	SU6	387510.5	3789907.5	1492.8	1489.4	753.3	748.5	1.4	0.6	0.27	0.51	16.31	4.80
Sutton Canyon	SU7	387489.5	3789897.5	1467.1	1465.1	745.8	744.1	1.4	0.6	0.12	0.18	24.31	1.65
Vogel Canyon	V1	388403.5	3797178.5	4237.8	4233.4	991.2	984.4	1.4	1.0	N.D.	N.D.	N.D.	N.D.
Vogel Canyon	V2	388125.5	3796784.5	3405.0	3396.2	908.0	892.6	1.6	0.8	0.09	0.11	837.16	15.36
Vogel Canyon	V3	388100.5	3796791.5	3365.5	3360.7	888.6	881.2	1.6	0.8	0.13	0.32	35.56	7.34
Vogel Canyon	V4	387851.5	3796716.5	3010.4	3003.9	852.8	846.6	2.2	0.7	0.08	0.10	356.71	6.21
Vogel Canyon	V5	387846.5	3796705.5	2997.3	2979.6	845.1	810.3	2.2	0.7	0.22	1.49	24.31	34.78
Vogel Canyon	V6	387850.5	3796613.5	2867.4	2863.6	803.2	800.0	2.2	0.7	0.06	0.09	116.05	3.27
Vogel Canyon	V7	387865.5	3796610.5	2849.5	2845.7	798.7	796.1	2.2	0.7	0.09	0.22	17.90	2.59
Vogel Canyon	V8	387871.5	3796606.5	2841.9	2838.0	795.6	792.4	2.2	0.7	0.12	0.49	7.66	3.26
Vogel Canyon	V9	387761.5	3796502.5	2634.8	2620.7	774.1	745.2	2.3	0.6	0.09	0.22	217.28	28.86
Vogel Canyon	V10	387422.5	3795447.5	844.1	841.2	638.5	636.7	4.3	0.2	0.06	0.06	1779.51	1.81
Vogel Canyon	V11	387448.5	3795364.5	720.6	711.4	630.3	619.0	4.3	0.2	0.05	0.14	129.88	11.29
Ybarra Canyon	Y1	387007.5	3797414.5	3886.8	3881.6	942.3	934.9	1.0	1.0	N.D.	N.D.	N.D.	N.D.
Ybarra Canyon	Y2	387073.5	3797354.5	3784.6	3779.3	922.7	917.6	1.1	0.9	0.13	0.17	102.23	5.11
Ybarra Canyon	Y3	387082.5	3797324.5	3750.0	3744.6	910.9	903.7	1.1	0.9	0.23	0.40	34.73	7.21
Ybarra Canyon	Y4	387092.5	3797270.5	3687.4	3684.4	896.0	893.7	1.1	0.9	0.13	0.17	60.21	2.37
Ybarra Canyon	Y5	387079.5	3797189.5	3585.8	3581.8	884.0	879.7	1.1	0.9	0.10	0.14	102.60	4.28
Ybarra Canyon	Y6	387050.5	3797181.5	3553.5	3551.1	877.3	875.6	1.1	0.9	0.09	0.13	30.73	1.66
Ybarra Canyon	Y7	387028.5	3797162.5	3522.5	3520.5	869.1	867.2	1.1	0.9	0.23	0.27	30.63	1.89
Ybarra Canyon	Y8	386913.5	3797015.5	3302.9	3297.7	837.3	833.1	1.2	0.8	0.14	0.15	222.76	4.23
Ybarra Canyon	Y9	386755.5	3796801.5	2993.9	2990.5	796.1	792.1	1.8	0.7	0.12	0.13	307.23	4.08
Ybarra Canyon	Y10	386763.5	3796781.5	2969.4	2965.0	789.4	785.1	1.8	0.7	0.13	0.27	25.49	4.27
Ybarra Canyon	Y11	386769.5	3796744.5	2925.7	2922.7	777.9	775.9	1.8	0.7	0.18	0.22	42.31	1.97
Ybarra Canyon	Y12	386694.5	3796683.5	2812.0	2805.8	758.8	750.8	1.8	0.7	0.16	0.22	116.88	8.00
Ybarra Canyon	Y13	386689.5	3796671.5	2797.9	2793.1	749.4	744.7	1.8	0.7	0.17	0.48	12.66	4.71
Ybarra Canyon	Y14	386623.5	3796591.5	2661.8	2657.8	726.7	722.8	3.4	0.7	0.14	0.16	135.30	3.95
Ybarra Canyon	Y15	386594.5	3796607.5	2620.8	2618.0	718.5	716.5	3.4	0.7	0.12	0.16	39.87	2.03
Ybarra Canyon	Y16	386542.5	3796561.5	2524.5	2519.5	705.3	698.5	3.4	0.6	0.12	0.18	98.50	6.73
Ybarra Canyon	Y17	386503.5	3796544.5	2466.2	2463.2	693.8	691.6	3.4	0.6	0.09	0.12	56.28	2.22
Ybarra Canyon	Y18	386281.5	3796440.5	2084.2	2074.8	664.2	651.1	3.7	0.5	0.07	0.10	388.36	13.14
Ybarra Canyon	Y19	387625.5	3797160.5	4236.2	4230.3	916.2	909.5	1.0	1.0	N.D.	N.D.	N.D.	N.D.
Ybarra Canyon	Y20	387272.5	3796999.5	3729.4	3724.1	875.9	871.7	1.2	0.9	0.07	0.07	506.22	4.20
Ybarra Canyon	Y21	387049.5	3796891.5	3381.4	3378.9	838.3	836.0	1.5	0.8	0.10	0.10	345.19	2.28
Ybarra Canyon	Y22	387023.5	3796888.5	3351.6	3345.4	832.5	823.5	1.5	0.8	0.13	0.37	33.56	9.01
Ybarra Canyon	Y23	387000.5	3796867.5	3316.4	3312.4	820.5	817.1	1.5	0.8	0.10	0.19	32.97	3.40
Ybarra Canyon	Y24	386948.5	3796817.5	3235.8	3232.4	811.7	808.2	1.5	0.8	0.07	0.11	79.98	3.46
Ybarra Canyon	Y25	386946.5	3796812.5	3230.0	3227.0	806.8	804.2	1.5	0.8	0.57	0.73	5.41	2.60
Ybarra Canyon	Y26	386857.5	3796677.5	3014.8	3012.4	788.4	786.6	1.5	0.7	0.07	0.08	214.59	1.78
Ybarra Canyon	Y27	386856.5	3796649.5	2983.1	2980.3	783.6	781.9	1.5	0.7	0.10	0.15	32.14	1.68
Ybarra Canyon	Y28	386713.5	3796586.5	2791.6	2789.2	764.0	761.8	1.5	0.7	0.09	0.11	191.07	2.19
Ybarra Canyon	Y29	386665.5	3796581.5	2725.28	2707.03	754.7	732.0	1.5	0.6	0.11	0.36	82.18	22.76

Note: N.D. stands for No Data

*X_L is the horizontal distance of the waterfall lip from the outlet.

**X_B is the horizontal distance of the waterfall base from the outlet.

#Z_L is the elevation of the waterfall lip.

##Z_B is the elevation of the waterfall base.

###Non-dimensional distance of waterfalls calculated as the distance from the outlet divided by the total length of stream.

*#S_R is the slope of the river excluding relief from waterfalls measured for the reach above each waterfall unit.

**#S_U is the waterfall unit slope measured from the base of the upstream waterfall to the base of the downstream waterfall.

+L_U is the waterfall unit length measured as the horizontal distance from the base of the upstream waterfall to the base of the downstream waterfall.

++H_{wf} is the height of the waterfall step measured from lip to base.

SUPPLEMENTAL MATERIALS

Supplemental Methods

Influence of Threshold Values on Waterfall Metrics

I identified waterfalls using three threshold variables: a threshold drainage area set to 1 km^2 to identify the location of the channel head, a threshold waterfall slope set to 30°, and a threshold step height set to 1.5 m. I evaluated the influence of these thresholds on the results by repeating the analyses and individually varying each of the three threshold values. I examined the impact of using a threshold drainage area of 2 km^2 and 0.5 km^2 (Fig. S2), a threshold step height of 1 m and 2 m (Fig. S3), and threshold step slope of 25° and 40° (Fig. S4). In all cases, changes to the threshold values do not result in large changes to the results, and do not change the primary interpretations (Figs. S2-4).

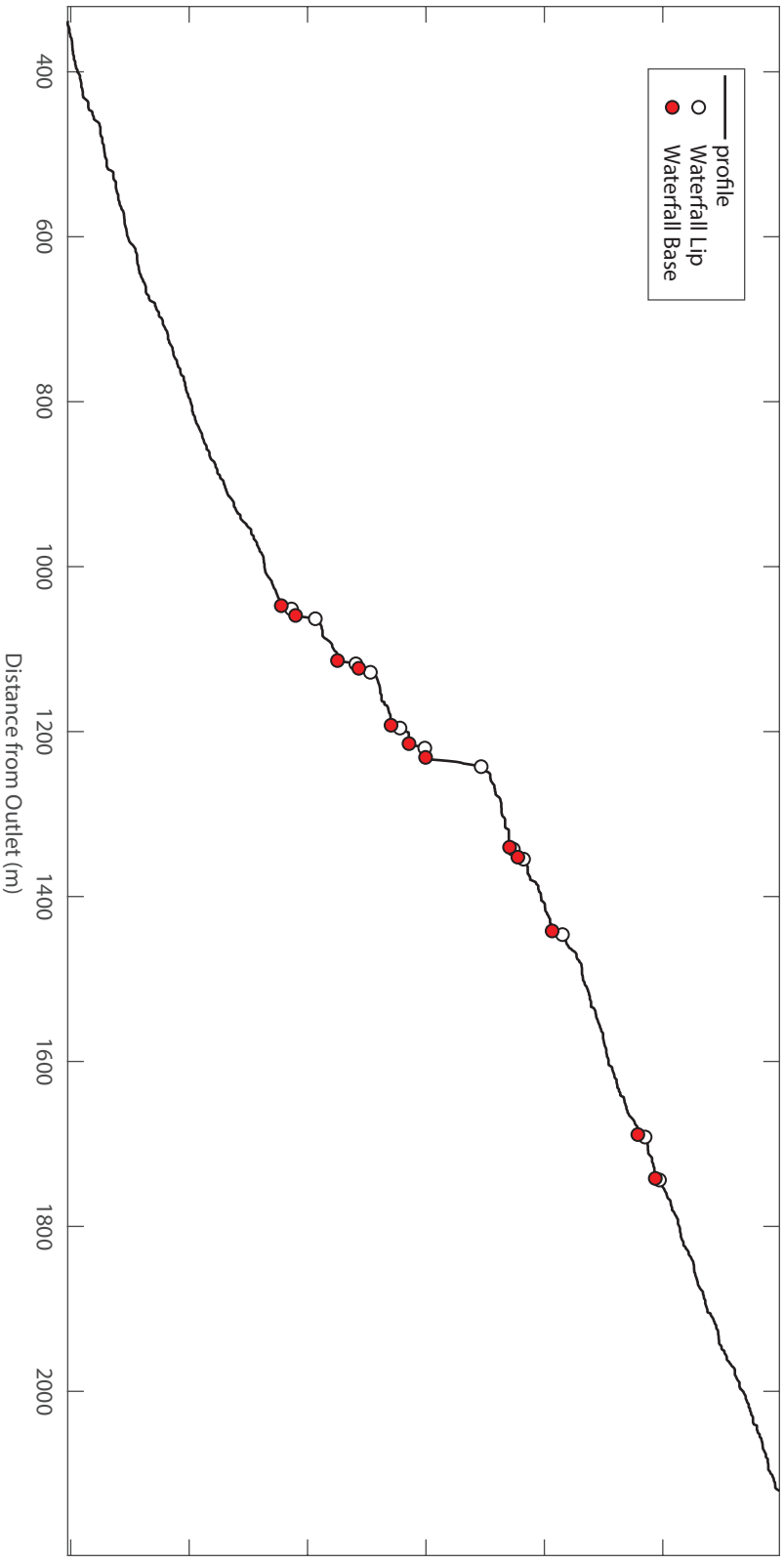

Figure S1: Example of profile with waterfall tops and bottoms indicated. This is the output of the waterfall identification code.

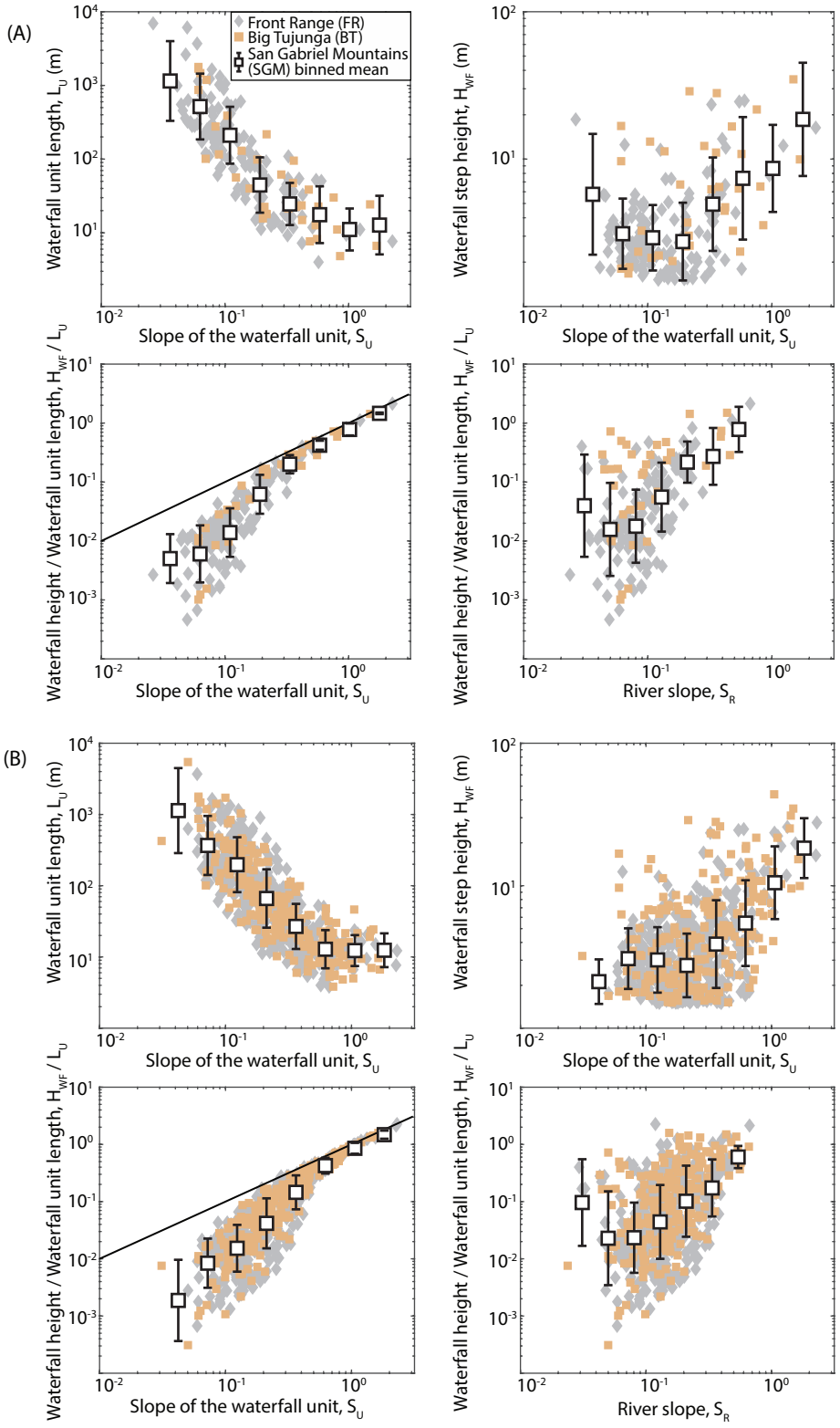

Figure S3: Plot of waterfall metrics versus slope varying threshold drainage area from (A) 2 km^2 to (B) 0.5 km^2 while holding threshold step height and slope constant at 1.5 m and 30°, respectively.

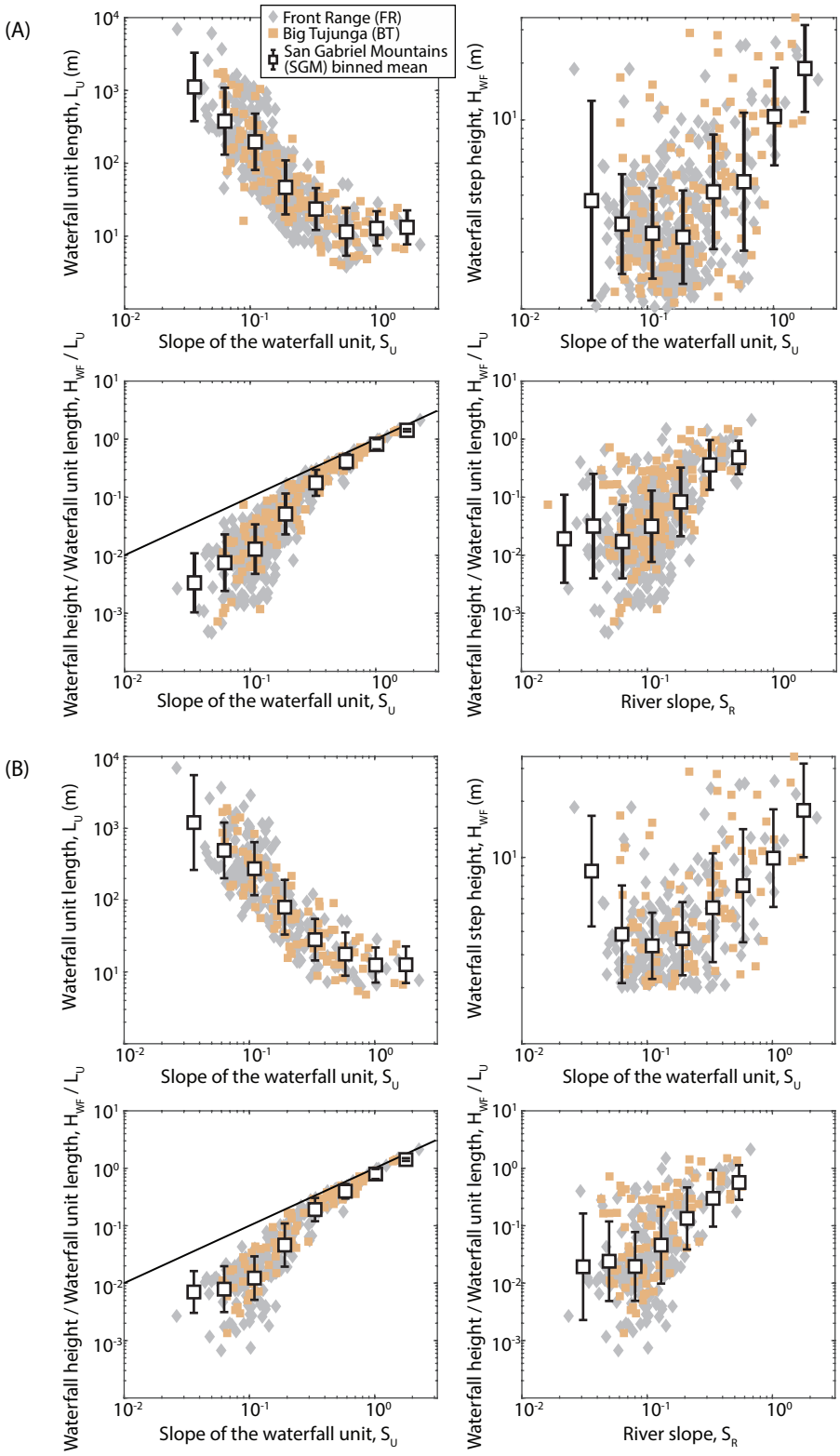

Figure S3: Plot of waterfall metrics versus slope varying threshold step height from (A) 1 m to (B) 2 m while holding threshold drainage area and slope constant at 1 km^2 and 30°, respectively.

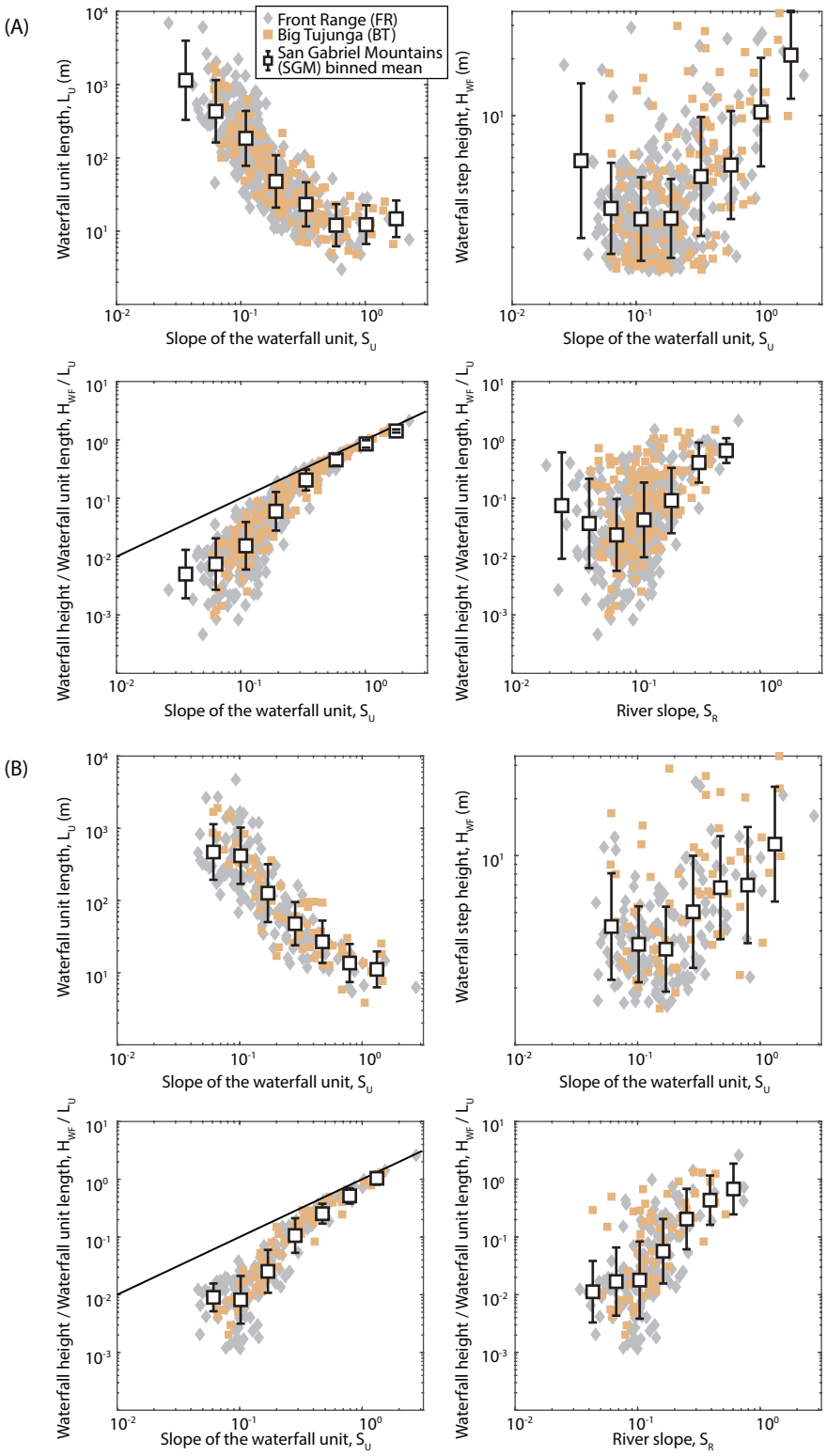

Figure S4: Plot of waterfall metrics versus slope varying threshold slope from (A) 25° to (B) 40° while holding threshold step height and drainage area constant at 1.5 m and 1 km^2, respectively.

```
clc, clear all, close all

%First set the threshold inputs
A = 1e6; %sets the threshold drainage area for what is defined as a channel from the DEM
(m^2)
dh = 1.5; %sets the theshold waterfall height (vertical distance between waterfall lip
and base) (m)
s = 30; %sets the threshold waterfall slope (sets of 3 pixels must be above this slope)
(degrees)

%Run the code to generate the river long profile from TopoToolbox
[P_Rubio] = profile_generator('Rubio_DEM.tif',A,'Rubio'); %uses the DEM created in ArcGIS
and saved in .tif format, the threshold drainage area set above, and the name of the
watershed
%produces a DEM hillshade of the watershed with the trunk channel


%Run the code to pick out waterfalls and calculate the morphologic metrics
[WF_Rubio] = wf_finder(P_Rubio,s,dh,'Rubio'); %uses the output from the function above,
the threshold waterfall slope and height set above, and the name of the watershed
%produces a profile with the waterfalls plotted on it
```

```
function [P] = profile_generator(DEM_fname,thresh_A,name)
%Function to create a profile from a DEM

%Add the folders where TopoToolbox and the DEMs are saved
addpath(genpath('D:\MATLAB\topotoolbox-master')) %path to where TopoToolbox is saved
addpath D:\MATLAB\GIS_Data\San_Gabriel_Mnts\Clipped_DEMs_tif %path to where DEMs are saved (must be in tif format)

DEM = GRIDobj(DEM_fname); %general variable for DEM, creates a grid object

FD = FLOWobj(DEM,'preprocess','carve'); %caclculate flow direction and carve the DEM to remove holes

DEMc = imposemin(FD,DEM); %create new carved DEM using the above output FD

A = flowacc(FD).*(FD.cellsize^2); %Calculate flow accumulation and make A give drainage area in m2 instead of # of pixels
A_thresh = thresh_A./(FD.cellsize^2); % upper drainage area threshold (in m^2), sets the channel head location - everything with smaller drainage is not counted as a stream

S = STREAMobj(FD,'minarea',A_thresh); %define the stream network

S_largest = klargestconncomps(S); %extract the largest connected stream network
S_trunk = trunk(S_largest); %extract the trunk of the stream network (the longest channel in the network)

MS = STREAMobj2mapstruct(S_largest); %Create a map structure of the river network to save as a shapefile for loading into ArcGIS

[lat,long,elev,dist,area] = STREAMobj2XY(S_largest,DEMc,S_largest.distance,A); %extract the variables of interest

%calculate the slope at each pixel along the channel
slope = zeros(size(dist));
slope(:) = NaN;

for i = 2:(length(dist)-1)
    slope(i) = (elev(i-1)-elev(i+1))./(dist(i-1)-dist(i+1)); %slope is rise over run for each pixel
end

slope_deg = atand(slope); %convert slope to degrees

%%
%combine all of the variables into one for output
P.x = lat;
P.y = long;
P.d = dist;
P.z = elev;
P.a_m = area;
P.s = slope;
```

```
P.s_deg = slope_deg;
P.MS = MS; %this saves the map structure of the stream network for uploading into ArcGIS
%%
%Plot a hillshade of the DEM with the main stem overlain on it
figure
imageschs(DEM, DEM, 'colorbarylabel', 'Elevation (m)')
hold on
plot(S_trunk,'r-', 'linewidth', 2)
title({'Entire stream network ',name})
xlabel('UTM Easting (m)')
ylabel('UTM Northing (m)')
```

```
function [WF] = wf_finder(P,thresh_slope,thresh_dh,name)
%function that finds waterfalls and their metrics

%Meet the first condition (slope over threshold value):
thresh_slope_i = P.s_deg > thresh_slope; %this creates an index with values 0 = false and
1 = true if slope is over threshold for each location along the profile

diff_slope_i = diff(thresh_slope_i); %this finds the difference of each value in the
index minus the value before it which means there will be a 1 where the index
%goes from 0 to 1 and a -1 where the index goes from 1 to 0 so
%groups of 1 values in the slope index will be bounded by a 1 and -1 (1 at
%the top of the wf and -1 at the bottom of the wf)

diff_slope_i = [NaN; diff_slope_i];

%define the top and bottom of waterfalls as wherever there are multiple points together
over the threshold slope
i_bottom = diff_slope_i == -1;
i_top = diff_slope_i == 1; %this selects the values in the index (of diffence between
slopes over threshold)that are either 1 or -1

z_bottom = P.z(i_bottom);
z_top = P.z(i_top); %this assigns the locations of the 1 and -1 values to the actual
elevation on the profile

dist_bottom = P.d(i_bottom);
dist_top = P.d(i_top); %this assigns the locations of the 1 and -1 values to the distance
from outlet on the profile

%define waterfall height
dh = abs((z_bottom) - (z_top)); %this takes the elevation point at the top of the
waterfall minus the bottom to get the change in height between them (i.e. height of
waterfall)

%Meet the second condition (dropheight over threshold):
i_dhover = dh > thresh_dh;
wf_dh = dh(i_dhover); %this is saying there is a waterfall by given definition where the
drop height is greater than the threshold value input

%Find the top (lip) and bottom (base) of the waterfall
wf_dist_bot = dist_bottom(i_dhover);
wf_dist_top = dist_top(i_dhover);

wf_z_bot = z_bottom(i_dhover);
wf_z_top = z_top(i_dhover);

%Get the drainage area at each waterfall
DA_top = P.a_m(i_top);
Awf = DA_top(i_dhover); %drainage area at each wf top in m^2

%Calculate number of waterfalls on each channel
```

```
count_wfs = length(wf_z_top);

%find the UTM locations of the waterfall tops
x_top = P.x(i_top);
y_top = P.y(i_top);

wf_x_top = x_top(dh>thresh_dh); %x is UTM East
wf_y_top = y_top(dh>thresh_dh); %y is UTM North


%Calculate the metrics of waterfall morphology
Su = zeros(size(wf_dist_bot));
Su(:) = NaN;
Lu = Su;
Hwf = Su;
Sr = Su;

for i=2:length(wf_dist_bot)
    Su(i) = (wf_z_bot(i-1) - wf_z_bot(i)) ./ (wf_dist_bot(i-1) - wf_dist_bot(i)); %Slope of the waterfall unit: calculated from the base of a waterfall to the base of the next downstream waterfall
    Sr(i) = (wf_z_bot(i-1) - wf_z_top(i)) ./ (wf_dist_bot(i-1) - wf_dist_top(i)); %River slope (excluding waterfalls): calculated from the base of a waterfall to the lip of the next downstream waterfall
    Lu(i) = wf_dist_bot(i-1) - wf_dist_bot(i); %Length of the waterfall unit: Includes the waterfall and section above it to the base of the upstream waterfall
    Hwf(i) = wf_dh(i); %waterfall height (excludes the upstream-most waterfall)
end

Hwf2Lu = Hwf ./ Lu;

%%
%Combine the variables into one output
WF.count_wfs = count_wfs;
WF.UTME_wf_top = wf_x_top;
WF.UTMN_wf_top = wf_y_top;
WF.dist_bot = wf_dist_bot;
WF.dist_top = wf_dist_top;
WF.z_bot = wf_z_bot;
WF.z_top = wf_z_top;
WF.A = Awf;
WF.Lu = Lu;
WF.Hwf = Hwf;
WF.Hwf2Lu = Hwf2Lu;
WF.Su = Su;
WF.Sr = Sr;
%%
%Plot the profiles with the waterfall lip and base
figure
plot(P.d,P.z,'k-','LineWidth',1,'DisplayName','profile')
hold on
```

```
plot(wf_dist_top,wf_z_top,'ko','markerfacecolor','w','DisplayName','Waterfall↙
Lip','markersize',6)
plot(wf_dist_bot,wf_z_bot, 'ko','markerfacecolor','r','DisplayName','Waterfall↙
Base','markersize',6)
title(name)
xlabel('Distance from Outlet (m)')
ylabel('Elevation (m)')
legend
```